

1 **Short title:** Proteogenomics of rice genome coding ability

2

3 **Corresponding authors:**

4 Liu Ying-Gao, State Key Laboratory of Crop Biology, College of Life Science,
5 Shandong Agricultural University, Taian, Shandong, China liuyg@sdau.edu.cn
6 Tel.: (86) 538 8249767

7 Zhang Jianhua, Department of Biology, Hong Kong Baptist University, and State Key
8 Laboratory of Agrobiotechnology, The Chinese University of Hong Kong, Shatin,
9 Hong Kong. jzhang@hkbu.edu.hk Tel.: (852) 3411 7011

10

11 **Full-length transcript-based proteogenomics of rice improves its genome and**
12 **proteome annotation**

13

14 Mo-Xian Chen^{a,c,1}, Fu-Yuan Zhu^{b,1}, Bei Gao^{d,1}, Kai-Long Ma^{e,1}, Youjun Zhang^{f,g},
15 Alisdair R. Fernie^{f,g}, Xi Chen^h, Lei Daiⁱ, Neng-Hui Ye^c, Xue Zhangⁱ, Yuan Tian^a, Di
16 Zhang^d, Shi Xiaoⁱ, Jianhua Zhang^{j,2} and Ying-Gao Liu^{a,2}

17

18 ^a State Key Laboratory of Crop Biology, College of Life Science, Shandong
19 Agricultural University, Taian, Shandong, China.

20 ^b Co-Innovation Center for Sustainable Forestry in Southern China, College of Biology
21 and the Environment, Nanjing Forestry University, Nanjing, China.

22 ^c Shenzhen Institute of Synthetic Biology, Shenzhen Institutes of Advanced
23 Technology, Chinese Academy of Sciences, Shenzhen 518055, P. R. China. ^d School
24 of Life Sciences, The Chinese University of Hong Kong, Shatin, Hong Kong.

25 ^e BGI-Shenzhen, Shenzhen, P. R. China.

26 ^f Max-Planck-Institut für Molekulare Pflanzenphysiologie, Am Mühlenberg 1, 14476
27 Potsdam-Golm, Germany.

28 ^g Center of Plant System Biology and Biotechnology, 4000 Plovdiv, Bulgaria.

29 ^h SpecAlly Life Technology Co., Ltd, Wuhan, China.

30 ⁱ State Key Laboratory of Biocontrol, Guangdong Provincial Key Laboratory of Plant
31 Resources, School of Life Sciences, Sun Yat-sen University, Guangzhou 510275,
32 China

33 ^j Department of Biology, Hong Kong Baptist University, and State Key Laboratory of
34 Agrobiotechnology, The Chinese University of Hong Kong, Shatin, Hong Kong.

35 ¹These authors contributed equally to this work.

36 ²To whom correspondence should be addressed. Email: liuyg@sdau.edu.cn and
37 jzhang@hkbu.edu.hk

38

39 **One sentence summary:** A full-length transcriptome-based proteogenomic dataset
40 reveals the complexity of rice gene arrangement and the transcriptome's coding ability.

41

42 **ABSTRACT**

43 Rice (*Oryza sativa*) molecular breeding has gained considerable attention in recent
44 years but inaccurate genome annotation hampers its progress and functional studies of
45 the rice genome. In this study, we applied single-molecule long-read RNA sequencing
46 (lrRNA_seq)-based proteogenomics to reveal the complexity of the rice transcriptome
47 and its coding abilities. Surprisingly, approximately 60% of loci identified by
48 lrRNA_seq are associated with natural antisense transcripts (NATs). The high-density
49 genomic arrangement of NAT genes suggests their potential roles in the multifaceted
50 control of gene expression. In addition, a large number of fusion and intergenic
51 transcripts have been observed. Furthermore, a total of 906,456 transcript isoforms
52 were identified, and 72.9% of the genes can generate splicing isoforms. 706,075
53 post-transcriptional events were subsequently categorized into ten subtypes,
54 demonstrating the interdependence of post-transcriptional mechanisms that contribute
55 to transcriptome diversity. Parallel short-read RNA sequencing indicated that
56 lrRNA_seq has a superior capacity for the identification of longer transcripts. In
57 addition, over 190,000 unique peptides belonging to 9,706 proteoforms/protein groups
58 were identified, expanding the diversity of the rice proteome. Our findings indicate that
59 the genome organization, transcriptome diversity, and coding potential of the rice
60 transcriptome are far more complex than previously anticipated.

61

62 **Keywords:** alternative splicing, alternative translation initiation, fusion, natural
63 antisense transcript, *Oryza sativa*, proteogenomics.

64

65

66 INTRODUCTION

67 Rice (*Oryza sativa*) is a model monocot and one of the most important crop
68 species globally. Functional studies using rice cultivars have been largely facilitated
69 by the release of its genome sequences and subsequent transcriptomic profiling
70 (Ouyang et al., 2007). The representative *japonica* (*geng*) rice genome was released in
71 the early 21st century, and initial genome annotation was based on multiple
72 approaches including *ab initio* prediction, paralog comparison, and transcript libraries
73 (e.g., cDNA and expressed sequence tags) (Ouyang et al., 2007). In recent years, this
74 annotation has been continuously updated using next-generation sequencing
75 (short-read RNA sequencing, srRNA_seq)-based transcriptome datasets in popular
76 databases such as Phytozome (Ouyang et al., 2007; Wang et al., 2018).

77 When srRNA_seq became widespread during the past decade, pervasive
78 transcription, a mechanism originally defined to generate unknown non-coding RNAs,
79 has been proposed for nearly all sequenced species (Mills et al., 2016). The
80 complexity of the RNA landscape revealed by high-throughput sequencing techniques
81 came as a major surprise. In particular natural antisense transcripts (NATs), which
82 were initially regarded as transcriptional noise, are amongst the most interesting
83 elements (Mills et al., 2016). NATs are defined as a pair of transcription units located
84 in different strands of DNA with overlapping loci coordinates (Pelechano and
85 Steinmetz, 2013). This type of genomic organization was initially identified in viruses
86 in 1969 (Bøvre and Szybalski, 1969) and was subsequently observed to be a common
87 feature in prokaryotic bacteria and eukaryotic organisms (Wek and Hatfield, 1986;
88 Wong et al., 1987). In recent years, comprehensive transcriptome studies have
89 revealed an ever-increasing percentage of loci involved in this genomic organization,
90 suggesting that NATs are highly prevalent in eukaryotes. According to current
91 research summary, approximately 50-70% of mammalian loci and 20-70% of plant
92 loci have antisense transcripts in the opposite strand (Katayama et al., 2005).

93 Although NATs have recently drawn increasing attention, their functional
94 significance is only just beginning to be understood (Xu et al., 2017). In addition, the
95 genomic arrangement of NATs reveals potential functional correlations between these
96 gene pairs (Pelechano and Steinmetz, 2013). For example, NATs have been
97 demonstrated to play crucial roles at both transcriptional and post-transcriptional
98 levels under a variety of abiotic and biotic stresses (Werner, 2005) with described
99 functions including roles in activating or silencing other members of NAT pairs
100 (Prescott and Proudfoot, 2002; Modarresi et al., 2012), mRNA processing and
101 splicing (Morrissy et al., 2011), the maintenance of RNA stability (Su et al., 2012),
102 the direction of chromatin remodelling (Swiezewski et al., 2009), induction of the
103 formation of siRNA (Borsani et al., 2005), and translational control (Faghihi and
104 Wahlestedt, 2009). Given the considerable number of NATs identified in animals and
105 plants, it is perhaps unsurprising that the biological functions of most NATs remain to
106 be elucidated by mechanistic studies.

107 In addition to NATs, specialized transcripts such as fusion genes have emerged
108 from transcriptome studies and opened a new research horizon. By definition, fusion
109 transcripts are chimeric mRNAs created by fusion of parts of different genes. Fusion
110 events commonly result from genomic translocation, chromosomal deletion, and
111 inversion, or *trans*-splicing mechanisms (Weirather et al., 2015). *Trans*-splicing,
112 which is often observed in lower eukaryotes, had been considered ‘rare’ in higher
113 eukaryotic organisms (McManus et al., 2010). To date, the cellular function of these
114 transcripts have been well characterized in mammalian tumorigenesis (Edwards, 2010;
115 Edwards and Howarth, 2012), however, cases in other higher eukaryotes, including,
116 plants are rarely reported.

117 In comparison to NATs and fusion genes, post-transcriptional regulation
118 methods such as alternative transcription start (ATS), alternative splicing (AS), and
119 alternative poly-adenylation (APA), as well as their resulting mRNA isoforms, have
120 been well established in recent years (Abdelghany et al., 2016; Wang et al., 2016). It

121 has been documented that 50% of genes have ATS, over 95% of genes exhibit AS,
122 and 75% of genes have APA in humans (Pan et al., 2008; Reddy et al., 2013).
123 Furthermore, approximately 15% of human diseases are caused by mutations that
124 affect splicing machinery (Eckardt, 2013). Hence, these three mechanisms are
125 proposed to interdependently expand the transcriptome coding ability and proteome
126 diversity based on the limited information stored in eukaryotic genomes (Abdelghany
127 et al., 2016). At the transcriptional level, the potential roles of ATS and APA in
128 delicately controlling translation efficiency and mRNA stability are well documented
129 (Reyes and Huber, 2018). Eukaryotic genes typically consist of multiple exon and
130 introns. In vertebrates, on average 7.8–9.0 introns per gene have been observed
131 (Mourier and Jeffares, 2003), suggesting that AS could greatly increase the repertoire
132 of translated proteins involved in every aspect of developmental and environmental
133 responses (Kalsotra and Cooper, 2011; Laloum et al., 2018). However, the question of
134 whether a transcribed mRNA isoform can be translated is still under open debate
135 (Tress et al., 2016). That said, a considerable number of isoforms have been found to
136 be associated with ribosome or proteins, as evidenced by proteomic studies,
137 suggesting their coding potential under normal conditions or stress treatment (Zhu et
138 al., 2017). Although a number of functional studies have characterized the mRNA
139 isoforms in animals and plants in order to reveal their potential roles in signal
140 transduction and cellular activities (Ruhl et al., 2012; Duan et al., 2016; Hwang et al.,
141 2018), the functional significance of the vast majority of isoforms remains poorly
142 understood. In addition to transcriptional and post-transcriptional control, eukaryotes
143 can further increase their coding potential to generate proteins or short peptides by
144 using alternative open reading frames (ORFs) or small ORFs located in the 2nd or 3rd
145 frame of the same transcript, respectively. These translational mechanisms are defined
146 as alternative translation initiation (ATI) (Sonenberg and Hinnebusch, 2009).
147 Additionally, the usage of non-AUG or non-canonical start codons has been
148 demonstrated by parallel analysis of ribosome sequencing and proteomic profiling,

149 further enhancing eukaryotic and prokaryotic genome coding potential, respectively
150 (Ingolia et al., 2011; Menschaert et al., 2013; Bouthier et al., 2015; Lomsadze et al.,
151 2018).

152 Proteogenomics is an analytical approach to integrate genomic, transcriptomic,
153 and proteomic data for comprehensive analysis. The first proteogenomic work was
154 carried out in *Arabidopsis* (*Arabidopsis thaliana*) for its genome annotation
155 (Castellana et al., 2008). Subsequently, this approach has been applied to the model
156 legume *Medicago truncatula* and grapevine (*Vitis vinifera*)(Volkening et al., 2012;
157 Chapman and Bellgard, 2017). Proteogenomics has been carried out not only in plants,
158 but also in animals and microorganisms (Jaffe et al., 2004; Locardpaulet et al., 2015;
159 Kumar et al., 2016). In addition to aiding the curation of genome annotation,
160 proteogenomics can be used to detect processed signal peptides, to identify
161 specialized transcripts and their protein products, to discover protein maturation
162 events, and to reveal leaderless mRNA and its mechanism during translation initiation
163 (De Groot et al., 2014; Kucharova and Wiker, 2015).

164 The aforementioned genomic features and specialized transcripts are efficiently
165 detected by srRNA_seq with sufficient sequencing depth. However, the main
166 limitation of this technology is the dependence on bioinformatic assembly of
167 transcripts from short sequencing reads (75-150 bp) by available computational tools
168 (Conesa et al., 2016). For instance, although srRNA_seq can accurately detect AS
169 events or splicing sites, it is challenging to determine the combinatory usage of
170 splicing junctions or assemble full-length transcript isoforms and fusion transcripts
171 using this method (Wang et al., 2016; Wang et al., 2018). Furthermore, the lengths of
172 transcripts assembled by srRNA_seq can be further limited by the computational
173 algorithm, which subsequently leads to inaccurate annotation of gene models and their
174 genomic coordinates. This seriously hampers the identification of NATs. With the
175 development of technology for single-molecule long-read RNA sequencing
176 (lrRNA_seq) from Pacific Biosciences (PacBio), researchers are now able to obtain

177 full-length transcripts as a single read without further assembly (Deveson et al., 2018).
178 Recent transcriptome studies have demonstrated the utility of this technology in
179 providing superior information on transcript isoforms in yeast, humans, and plants
180 (Sharon et al., 2013; Abdelghany et al., 2016; Wang et al., 2016; Kuang et al., 2017;
181 Wang et al., 2018). These studies have suggested that even in the highly characterized
182 human transcriptome, the identification of genes and splice isoforms is far from
183 complete (Sharon et al., 2013; Wang et al., 2016). In addition, most studies have been
184 inspired by the diversity and complexity of various types of transcripts, such as
185 splicing isoforms and fusion transcripts, or by post-transcriptional regulations such as
186 ATS and APA, and little attention has been paid to the study of genomic
187 arrangements, such as NATs. Furthermore, although studies have questioned the
188 coding potential of these transcripts, no direct experiments have been carried out.

189 Recent studies have applied srRNA_seq-based proteogenomics on rice and
190 lrRNA_seq for rice transcriptome analysis, respectively (Ren et al., 2019; Zhang et al.,
191 2019). In this study, we performed a comprehensive analysis of lrRNA_seq-based
192 transcriptome and proteomic datasets simultaneously to provide direct proteomic
193 evidence for rice. In order to systematically characterize transcript isoforms, we chose
194 six tissue types at different developmental stages from *japonica* (*geng*) rice
195 Nipponbare, including seeds, seedlings, roots, leaves, stems, and flowers, for library
196 construction and lrRNA_seq. Meanwhile, parallel srRNA_seq using an Illumina
197 HiSeq 4000 platform was carried out for comparison. We demonstrate that 58.5% of
198 the genes form NAT pairs and 72.9% of the genes have transcript isoforms,
199 respectively. This suggests that lrRNA_seq has a superior ability to reveal complex
200 genomic arrangements and transcriptome dynamics. Furthermore, the coding potential
201 and characteristics of the rice transcriptome and proteome were assessed using both
202 datasets alongside parallel qualitative proteomic experiments and data entries in
203 public databases. Our findings indicate that it is common for rice transcripts to not
204 only use all three frames to encode proteins, but to also use multiple transcripts to

205 encode a single protein. In summary, our data demonstrate that the
206 lrRNA_seq-assisted proteogenomic approach can be applied to eukaryotic organisms
207 in order to identify genomic arrangement, transcriptome diversity, and coding ability,
208 which complements current transcriptomic approaches and contributes to a better
209 understanding of the systems level control of a wide range of biological processes.

210

211

212 **RESULTS**

213 **Analytical pipeline of lrRNA_seq-based proteogenomics**

214 A schematic view of the analytical pipeline used in this study is shown in Figure
215 1, which was modified based on a previous study in Arabidopsis (Zhu et al., 2017).
216 Since transcripts of srRNA_seq and lrRNA_seq were assembled by different
217 bioinformatic pipelines (Supplemental Tables S1 and S2), we remapped the
218 assembled srRNA_seq transcripts together with lrRNA_seq transcripts using GMAP
219 (Abdel-Ghany et al., 2016) for normalization. The resulting gff files were used for
220 subsequent specialized transcript identification and comparison between these two
221 datasets. Pipeline refinements upon the identification of AS events, fusion and
222 intergenic transcripts, and NATs were conducted as detailed in the Materials and
223 Methods section. Proteomic profiling was conducted similarly to previous protocols
224 with minor modification by using a second digestion enzyme, Glu-C, as an
225 independent method to improve protein coverage. In addition, 24 protein datasets
226 deposited in the PRIDE archive were added for the subsequent peptide search. Due to
227 the usage of a strand-specific library, a three-frame library was constructed instead of
228 the 6-frame library used in previous studies, which consequently halved the
229 computing power required for the database search. Integrative analysis, such as
230 coding ability assessment and comparison between srRNA_seq and lrRNA_seq, was
231 carried out using methods custom-made for this study.

232

233 **General features and transcript identification**

234 To ensure the coverage and identification of low-abundance transcripts, both
235 srRNA_seq and lrRNA_seq were conducted with sufficient sequencing depth
236 (Supplemental Tables S1 and S2). In general, lrRNA_seq is superior to srRNA_seq in
237 transcript identification and characterization. A total of 120,958 and 1,100,036 unique
238 transcripts were identified by srRNA_seq and lrRNA_seq, respectively (Table 1).
239 Subsequently, 120,905 transcripts from srRNA_seq and 906,456 transcripts from

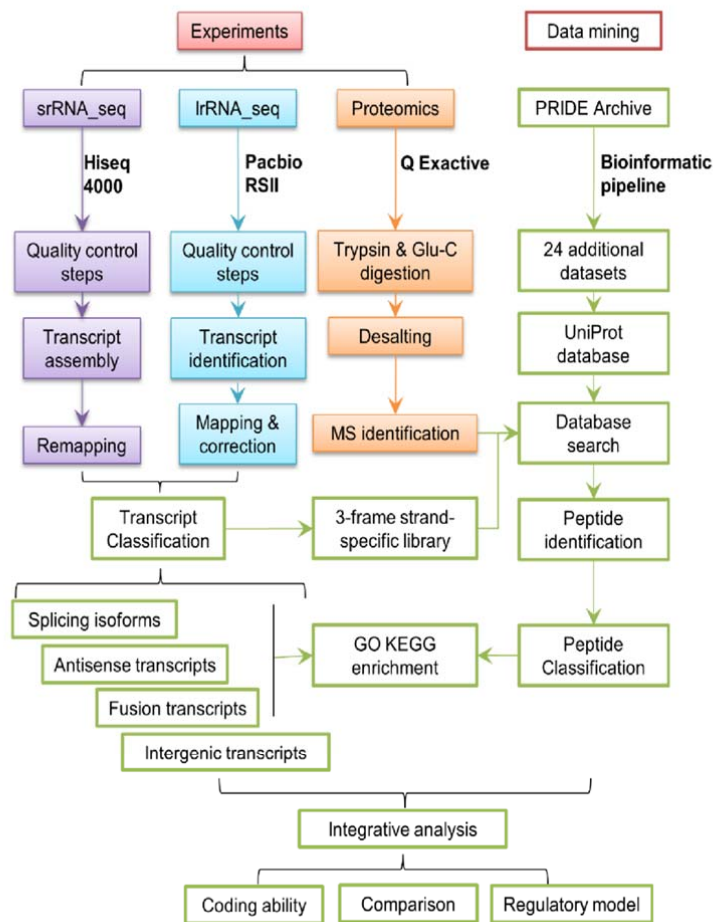


Figure 1 Schematic view of the experimental and analytical pipeline used in this study. srRNA_seq and lrRNA_seq was performed by using Hiseq 4000 and Pacbio RSII platform. Proteomic analysis was performed by using Q Exactive platform. Data mining was carried out by using online deposited datasets. Major steps of analytical pipeline are shown.

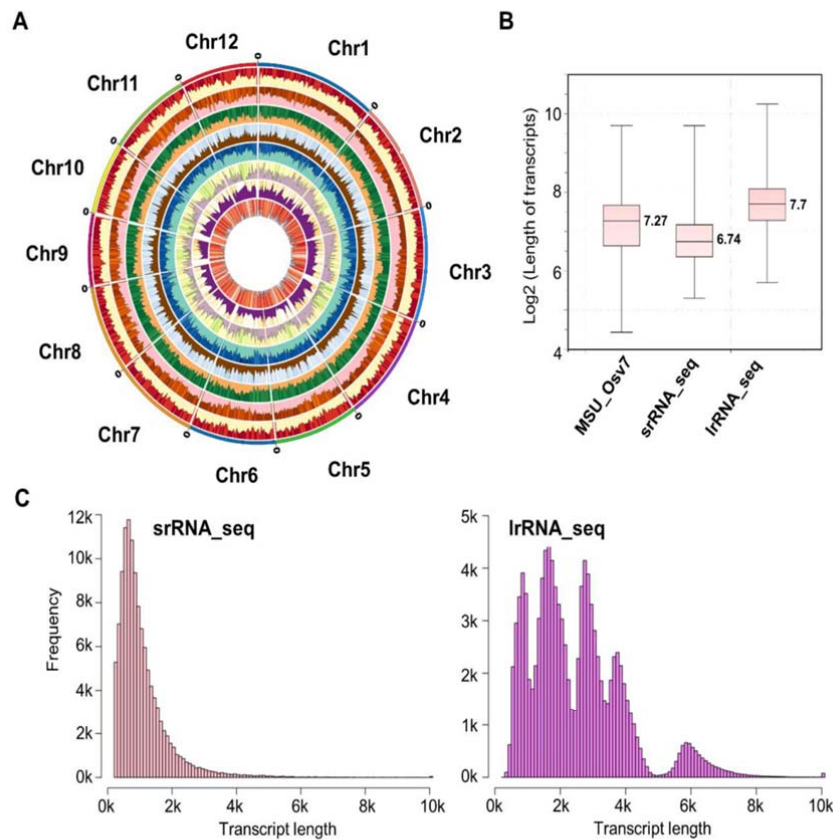


Figure 2 Comparison of transcript properties between srRNA_seq and lrRNA_seq. (A) Circos diagram of specialized transcripts identified by srRNA_seq and lrRNA_seq. 1, total transcripts identified by srRNA_seq; 2, total transcript identified by lrRNA_seq; 3, intergenic transcripts identified by srRNA_seq; 4, intergenic transcripts identified by lrRNA_seq; 5, NATs identified by srRNA_seq; 6, NATs identified by lrRNA_seq; 7, fusion transcripts identified by srRNA_seq; 8, fusion transcripts identified by lrRNA_seq. (B) Boxplot of transcript lengths summarized in the three datasets using MSU_Osv7 annotation, srRNA_seq and lrRNA_seq. Histogram plots showing the frequency of transcript lengths between (C) srRNA_seq and (D) lrRNA_seq.

242 detected 65,723 unannotated transcripts from 5,686 unannotated loci, whereas
243 lrRNA_seq identified 102,614 transcripts from 11,023 unannotated loci. For transcript
244 isoform identification, 6,384 loci with 16,617 splice isoforms were recorded in the
245 current rice annotation. srRNA_seq assembled 104,942 isoforms from 13,745 loci,
246 with 6,540 of these loci being present in the current rice annotation. lrRNA_seq
247 identified 867,136 isoforms from 32,780 loci, with over 8 times more transcripts and a
248 2.4-fold increase in loci characterization (Table 1). Additionally, 52,840 transcripts
249 from 7,205 unannotated loci and 65,942 transcripts from 7,505 unannotated loci were
250 identified by srRNA_seq and lrRNA_seq, respectively (Table 1). With regard to
251 specialized transcripts, lrRNA_seq identified 11 times, 6.5 times, and 3.6 times more
252 NATs, fusion transcripts, and intergenic transcripts than srRNA_seq, respectively
253 (Table 1). The genome-wide coverage and frequency of the aforementioned
254 transcripts are shown in a Circos diagram (Figure 2A). In addition to the advantage of
255 detecting a much greater number of transcripts, lrRNA seq was additionally better at
256 finding longer transcripts due to its longer read length. For example, the median value
257 of the transcript length from srRNA_seq was 845 bp, whereas this value reached 2206
258 bp for lrRNA_seq-identified transcripts (Figure 2B). This further increased the
259 median length of transcripts in the current rice annotation from 1435 to 2206 bp.
260 Similar results can be obtained by comparing the length distribution of the total
261 transcripts generated by both RNA_seq techniques (Figure 2C), suggesting that a
262 greater number of longer transcripts (>5 kb) were characterized using lrRNA_seq.

263

264 **Comparative analysis of fusion and intergenic transcripts**

265 Single-molecule transcriptome analysis in humans and plants has demonstrated
266 that transcript fusion events appear to be more common than previously thought
267 (Weirather et al., 2015; Wang et al., 2016). Given that these chimeric transcripts are
268 able to further expand the transcriptional diversity in eukaryotic genomes, we
269 additionally analysed fusion transcripts in our rice samples. The identification of fusion

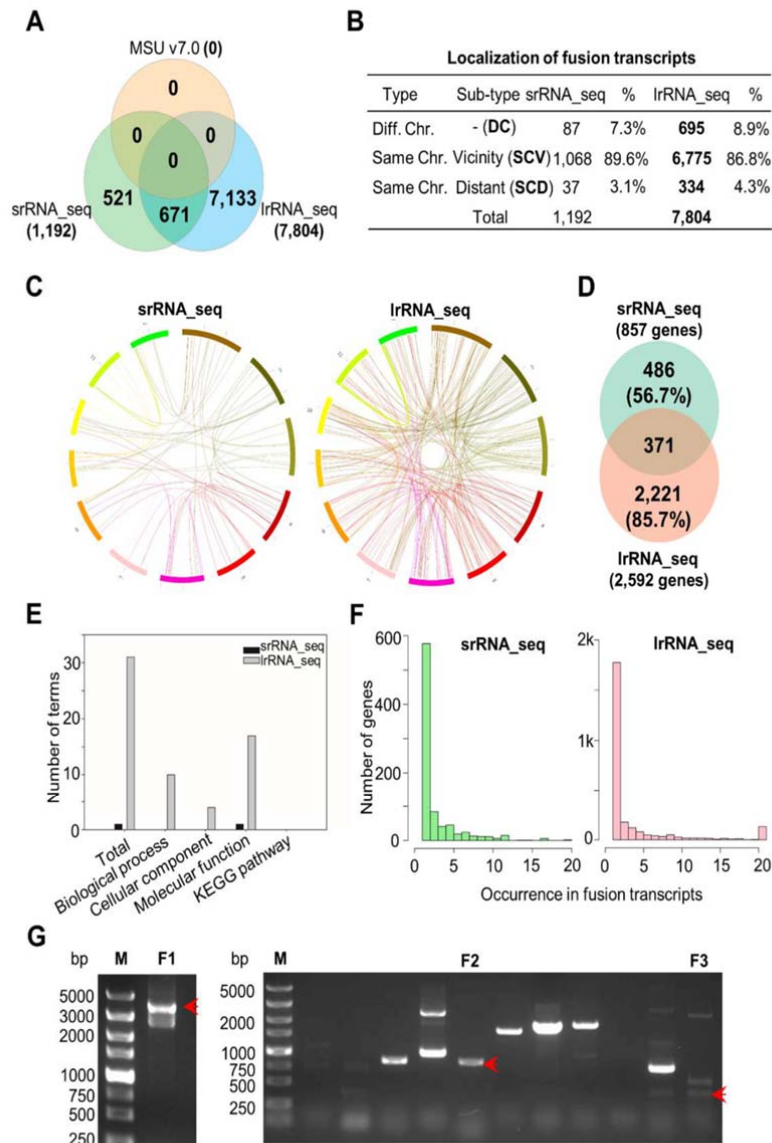


Figure 3 Comparative analysis of fusion transcripts.

(A) Venn diagram showing the overlapping and unique fusion transcripts identified by srRNA_seq and lrRNA_seq. (B) Summary of fusion transcript subtypes. (C) Circos representation of fusion transcripts consisting of two genes. (D) Venn diagram presenting the overlapping and unique genes involved in fusion transcript formation. (E) GO and KEGG enrichment analysis of fusion genes. (F) Loci frequency present in fusion transcripts. (G) RT-PCR validation of fusion transcripts. M, marker; bp, base pair; F1, F2, F3, three fusion transcripts.

1

270 events by srRNA_seq is questionable in its reliability due to the number of assembly

271 steps required. Although lrRNA_seq identified 7 times more fusions than did
272 srRNA_seq, a considerable amount of srRNA_seq-identified fusions were validated by
273 lrRNA_seq (Figure 3A). Subtype statistics revealed that most of the identified chimeric
274 transcripts (~90%) were intra-chromosomal fusions, resulting from the joining of two
275 adjacent genes (Figure 3B and Supplemental Figure S1A). Only a small proportion of
276 transcripts (~4%) and genes (~10 to 15%) were detected to be inter-chromosomally
277 fused by both sequencing approaches (Figure 3B and Supplemental Figure S1A),
278 which is similar to the results obtained previously in cancer cells (Okonechnikov et al.,
279 2016). Moreover, no preference of chromosome usage could be observed within the
280 identified fusion transcripts (Figure 3C). In total, 857 and 2,592 fusion-related genes
281 were identified, respectively, by srRNA_seq and lrRNA_seq, with approximately 56.7%
282 and 85.7% uniquely identified by each sequencing approach (Figure 3D). Among these
283 transcripts, the majority consisted of two genes, and approximately 1.5% and 2.8%
284 consisted of three genes in the srRNA_seq and lrRNA_seq datasets, respectively
285 (Supplemental Figure S1B). Furthermore, the internal organization of the fusion
286 transcripts determined using the sense or antisense strand varied between these two
287 datasets (Supplemental Figure S1C). With a higher number of identified transcripts,
288 more gene ontology (GO) terms were enriched in the lrRNA_seq dataset (Figure 3E
289 and Supplemental Table S3). In addition, some genes were found at a high frequency as
290 important building blocks for the construction of a variety of fusion transcripts (Figure
291 3F), and may hence play pivotal biological functions. Three fusion transcripts
292 identified by lrRNA_seq were validated by reverse transcription quantitative PCR
293 (RT-qPCR) and subsequent DNA sequence analysis (Figure 3G), confirming our
294 confidence of this approach in fusion transcript identification.

295 Intergenic transcripts are transcripts mapped to intergenic regions that are
296 frequently regarded to be non-coding transcripts (Chang et al., 2014). Interestingly
297 here the number of transcripts identified by the two methods was highly similar;
298 28,422 and 31,095 intergenic transcripts were identified by srRNA_seq and

299 lrRNA_seq, respectively. Their potential coding abilities were assessed by classic
300 long non-coding (lnc) RNA analysis. In general, 5,364 and 5,637 transcripts were
301 considered to be lncRNA according to previous descriptions (Supplemental Figure S2)
302 (Chang et al., 2014). However, determination of whether they can be translated or not
303 requires further protein evidence.

304

305 **Natural antisense transcripts reveal the complex linear arrangement of the rice** 306 **genome**

307 A previous report stated that by using tiling arrays, approximately 23.8% of
308 annotated rice genes could be identified as NATs (Li et al., 2006). Here using
309 innovative lrRNA_seq with its wide coverage of transcripts, we were able to classify
310 58.5% of the annotated genes as NATs (Table 1). A total of 2,603 and 10,414 NAT
311 genes identified by srRNA_seq and lrRNA_seq, respectively, overlapped with the
312 current rice annotation (Figure 4A). Furthermore, we summarized the previous
313 categorization of NATs into five subtypes based on their relative orientations and
314 regions of overlap (Figure 4B) (Yuan et al., 2015), including head-to-head (HTH),
315 tail-to-tail (TTT), embedded-1 (EMB-1), embedded-2 (EMB-2), and intronic (INT).
316 These five subtypes were further assessed at three levels including exon/intron pairs,
317 transcript pairs, and locus pairs (Figure 4C and Supplemental Figure S3A, B). Among
318 these, INT were the most abundant type in all three datasets, whereas the other four
319 subtypes were present in comparable percentages (Figure 4C and Supplemental Figure
320 S3A, B). In addition, a different statistical approach was used to characterize the NAT
321 subtypes as sense or antisense strands. No preference of strand usage for NATs was
322 observed in the lrRNA_seq dataset (Figure 4D). Although srRNA_seq-identified
323 NATs were uniquely enriched in several GO terms such as oxidoreductase, zinc ion
324 binding, and DNA binding, lrRNA_seq-identified NATs were much more enriched in
325 GO and the Kyoto Encyclopedia of Genes and Genomes (KEGG) terms (Figure 4E, F,
326 Supplemental Figure S3C, Supplemental Tables S4 and S5) due to the higher number

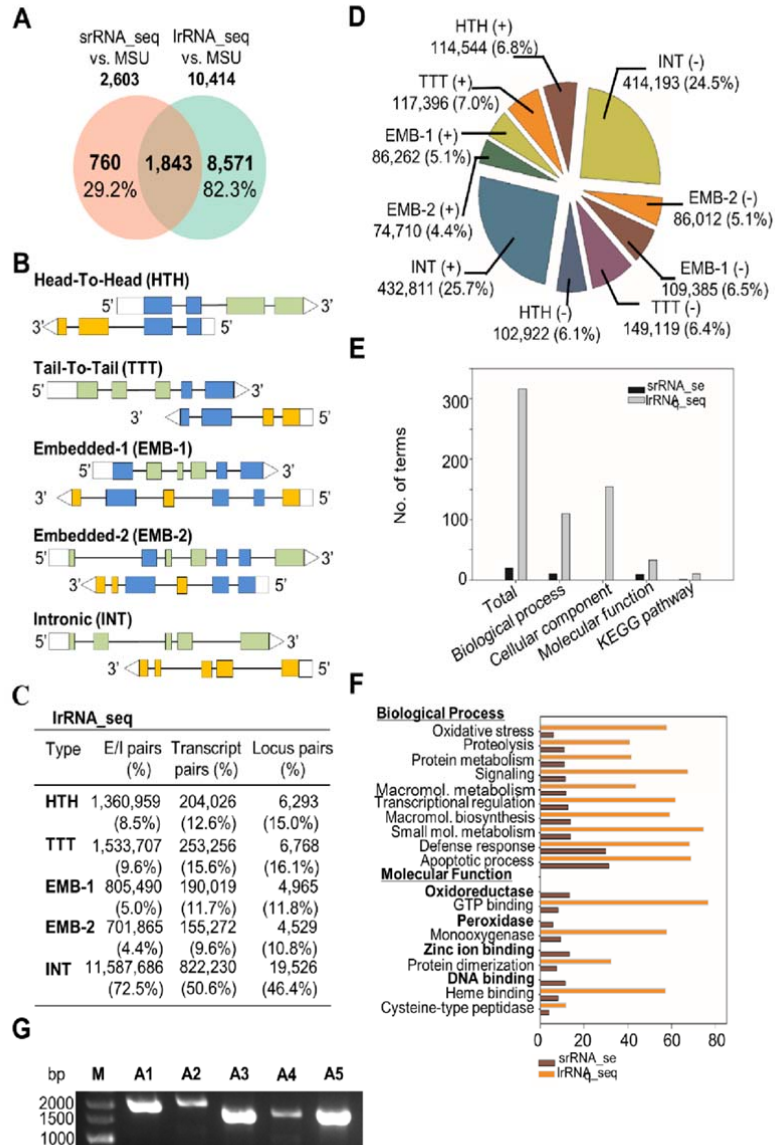


Figure 4 Comparison of natural antisense transcripts identified by srRNA_seq and lrRNA_seq. (A) Venn diagram showing the overlapped and unique transcripts present in the current annotation in comparison to the srRNA_seq and lrRNA_seq datasets. (B) Classification of 5 subtypes of NATs. (C) Summary of NATs identified by lrRNA_seq at the levels of exon/intron pairs, transcript pairs and locus pairs. (D) Summary of NAT subtypes in two strands of genomic DNA. (E, F) GO and KEGG enrichment analysis of NATs. (G) RT-PCR validation of antisense transcripts. M, marker; bp, base pair; A1-A5, antisense transcripts.

328 technology. Five of these transcripts were validated by an independent RT-qPCR
329 analysis (Figure 4G), proving the validity of our approach in the identification of
330 NATs.

331

332 **Diversity of post-transcriptional events and splicing site usage**

333 An increasing number of reports indicate that post-transcriptional (PT) events,
334 such as ATS, AS, and APA, are co-ordinately responsible for the majority of
335 transcript diversity (Reyes and Huber, 2018). As described previously, lrRNA_seq
336 presented the most diverse and abundant transcript isoforms in comparison to
337 srRNA_seq and the current rice genome annotation (Figure 5A). A total of 27,119 and
338 706,075 PT events were identified in the srRNA_seq and lrRNA_seq datasets,
339 respectively (Supplemental Figure S4). In comparison to srRNA_seq, the lrRNA_seq
340 results had a higher number of PT events both on a per transcript and per locus basis
341 (Supplemental Figure S4A). Previously, we proposed that two types of AS events,
342 named alternative first exon (AFE) and alternative last exon (ALE), are the two most
343 abundant AS events in rice and Arabidopsis (Zhu et al., 2017). Some of these AS
344 types were coordinated by non-AS events, such as ATS in AFE or APA in ALE. Thus,
345 we further defined these two events by removing events purely caused by ATS and
346 APA at diverse genomic positions (Supplemental Table S6), *i.e.*, AFE was a type of
347 PT event with coordinative effects between ATS and AS, whereas ALE was a
348 combined PT event with APA and AS. Hence, in addition to traditional AS types, ten
349 PT events were defined in this study to facilitate further analysis. Circos
350 representation suggested that lrRNA_seq was powerful for identifying these
351 genome-wide post-transcriptional events with a higher frequency and density than that
352 afforded by the srRNA_seq (Supplemental Figure 5B). However, the compositions of
353 these events varied between the two sequencing techniques. Four AS types, intron
354 retention (IR), multiple intron retention (MIR), exon skipping (SKIP), and multiple
355 exon skipping (MSKIP), were increased in percentage in the lrRNA_seq results

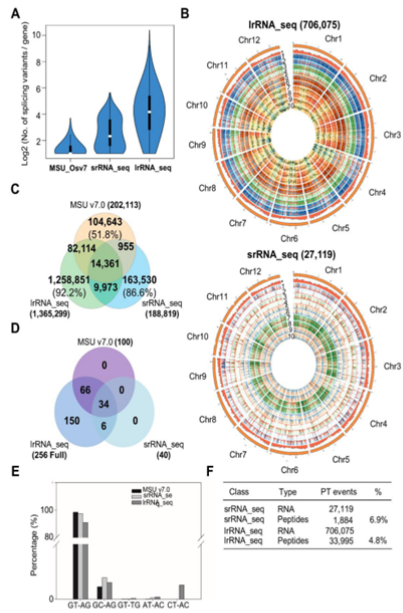


Figure 5 Identification of alternative transcription starts, alternative splicing and alternative polyadenylation.

(A) Violin plot of splicing variants identified in MSU_Os7 annotation, srRNA_seq and lrRNA_seq. (B) Circos representation of post-transcriptional events identified in srRNA_seq and lrRNA_seq. *, density of transcripts recorded in MSU_Os7 annotation; 1, intron retention (IR); 2, multiple intron retention (MIR); 3, exon

1

skipping (SKIP); 4, multiple exon skipping (MSKIP); 5, alternative exon 5' (AE5'); 6, alternative exon 3' (AE3'); 7, alternative transcript start (ATS); 8, alternative polyadenylation (APA); 9, alternative first exon (AFE); and 10, alternative last exon (ALE). Exon comparisons (C), paired splicing sites comparisons (D) and statistical analysis of paired splicing sites (E) among MSU_Os7 annotation, srRNA_seq and lrRNA_seq. (F) Summary of identified PT events and peptides in srRNA_seq and lrRNA_seq.

2

356 (Supplemental Figure S4B, C), suggesting that the longer read length of lrRNA_seq

357 may greatly facilitate the identification of these four AS types. By contrast, four PT
358 events including ATS, APA, AFE, and ALE were largely reduced in percentage
359 within the lrRNA_seq datasets (Supplemental Figure S4B, C), suggesting that they
360 were over-represented in the srRNA_seq due to the inability to detect all AS types.

361 In addition to alternative spliced isoform analysis, we further compared all exons
362 annotated in the three datasets (Supplemental Figure 5C). The current rice annotation,
363 srRNA_seq, and lrRNA_seq annotated 202,113, 188,819, and 1,365,299 exons,
364 respectively. Approximately 86.6% and 92.2% of exons were uniquely present in
365 datasets of srRNA_seq and lrRNA_seq, respectively (Supplemental Figure 5C),
366 highlighting the complexity of the post-transcriptional control of messenger RNA.
367 Traditionally, the choices of splice sites are recognized to strongly contribute to exon
368 variability (Zhu et al., 2017). Thus, we performed single splice site analysis to reveal
369 the genome-wide splice site conservation. Similar to previous results (Chen et al.,
370 2019b), the conventional 5'-splice site (5'-ss, GT) was present at approximately 60%
371 in both srRNA_seq and lrRNA_seq. However, the percentage of conventional 3'-ss
372 (AG) was largely reduced in the lrRNA_seq datasets, along with an increase in all
373 types of non-conventional 3'-ss sequences (Supplemental Figure S4D), implying that
374 these non-conventional 3'-ss are more likely to be detected in lrRNA_seq with its
375 longer read length. Thus, both 5'-ss and 3'-ss were less conserved (Supplemental
376 Figure S4E) than previously anticipated, suggesting a higher variability in the splice
377 choices than previously envisaged in eukaryotic genomes. Therefore, we employed a
378 paired splice site assay to locate 5'-ss / 3'-ss positions and sequences simultaneously
379 at a single intron. Findings from this analysis suggested that Phytozome annotation
380 exhibited 100 and srRNA_seq had 40 types of 5'-ss and 3'-ss sequence combinations
381 (Figure 5D). Surprisingly, all 256 combinations of splice site sequences were
382 observed in the lrRNA_seq dataset. Another interesting finding was that, besides
383 conventional U2 (GT-AG) and U12 complex (AT-AC), a third splicing combination
384 (GC-AG) accounted for a considerable percentage in all the splice sites identified in

385 this assay (Figure 5E). However, the underlying mechanisms and responsible protein
386 complex of this combination remain to be elucidated. Furthermore, proteomic
387 identification using the AS event library suggested that approximately 6.9% (1,884)
388 and 4.8% (33,995) of PT events identified from srRNA_seq and lrRNA_seq could be
389 translated to peptides (Figure 5F). This number is slightly lower in comparison to
390 previous examples reported in Arabidopsis and rice (Zhu et al., 2017; Chen et al.,
391 2019b).

392

393 **Proteogenomic analysis suggests multiple mechanisms for enhancing genome** 394 **coding ability**

395 The pervasive transcription of eukaryotic genomes has been documented for
396 years, but whether these transcripts can be translated is still a matter of debate (Jensen
397 et al., 2013; Wade and Grainger, 2014). To address this question, we conducted
398 large-scale profiling of the rice proteome to assess the potential coding ability of the
399 rice genome. Together with 24 previously published datasets (Supplemental Table S7),
400 a total of 7,368,042 spectra was included in the initial input file (Figure 6A).
401 Approximately 5.9% (464,969 spectra) was positively matched to peptide sequences
402 from a customized 3-frame translated database generated by combining both
403 srRNA_seq and lrRNA_seq transcripts (Figure 6A). In total, 9,706
404 proteoforms/protein groups (FDR<0.01) (Meier et al., 2018) were identified with at
405 least two peptide sequences (Figure 6A). In general, 191,862 peptides were found to
406 be translated from annotated loci and unannotated loci with at least two unique
407 peptide sequence(s) for each loci (Figure 6B) (Nesvizhskii, 2014). Among these, 92.6%
408 of the peptides were found to be regular proteins larger than 80 amino acids (Figure
409 6C), whereas approximately 6.6% of peptides belonged to small proteins between 11
410 to 80 amino acids and ~0.3% of peptides were from small peptides-encoding loci
411 (6-10 amino acids) (Figure 6C).

412

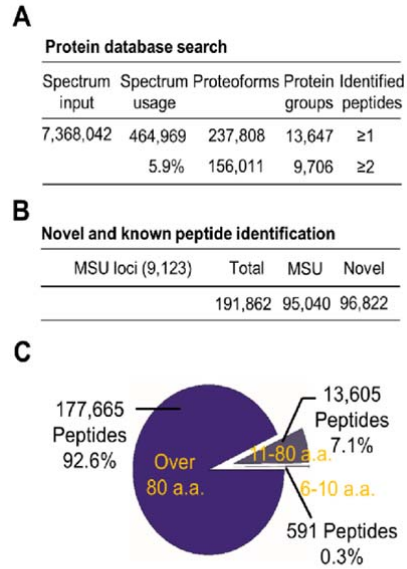


Figure 6 Assessment of coding potential by proteogenomics.

(A) Basic parameters used in proteomic database search. (B) Summary of known and unannotated peptides. (C) Distribution of identified proteoforms/protein groups and peptides.

414 **DISCUSSION**

415 In the past decade, srRNA_seq has become an essential technique for
416 characterizing eukaryotic transcriptomes. Given the complexity of eukaryotic
417 transcriptomes, using srRNA_seq is akin to putting pieces of a jigsaw together to see
418 the whole picture. Thus, the development of computational algorithms for reliable
419 full-length transcript reconstruction represents a major challenge (Steijger et al., 2013;
420 Tilgner et al., 2013). By contrast, lrRNA_seq has a number of advantages that may
421 allow it to supersede srRNA_seq. For example, the production of near full-length reads
422 greatly reduces the computing power required for transcript assembly. Simultaneously,
423 lrRNA_seq is powerful for revealing the higher complexity of eukaryotic genomes and
424 has become the gold standard for genome re-annotation due to its wide coverage of
425 full-length transcriptomes (Sharon et al., 2013; Wang et al., 2016). In addition, as
426 lrRNA_seq is a long-read-directed technology, it will facilitate the discovery of long
427 transcripts and low-abundance sequences (Wang et al., 2016). However, both
428 srRNA_seq and lrRNA_seq are able to uniquely identify a batch of transcripts (Figure
429 3A, Figure 4A, and Figure 5C). For this reason, we maximized the sampling diversity
430 by using rice samples at different developmental stages to ensure transcript coverage.
431 We also used srRNA_seq as a complementary dataset in parallel with the
432 lrRNA_seq-based proteogenomic analysis. In this way, we analysed the rice
433 transcriptome with sufficient depth and transcript length (Supplemental Tables S1 and
434 S2). This dataset has the potential to become a useful resource for studying
435 transcriptional and post-transcriptional regulation and genome annotation or to provide
436 database updates. This is exemplified by the fact that it allowed the discovery of a large
437 number of unannotated genes, along with their AS isoforms and coding proteins,
438 suggesting their authenticity as protein-coding loci. Furthermore, the expansion of the
439 transcript population may facilitate biological interpretation during developmental
440 processes and stress responses (Figure 3E and Figure 4E) by leading to the discovery of
441 unannotated structural or regulatory components of such processes.

442

443 **The universality of NATs implies high complexity and divergence in**
444 **transcriptional and post-transcriptional regulation**

445 Using srRNA_seq approaches, studies have demonstrated that NATs are universal
446 components of eukaryotic genomes (Balbin et al., 2015), participating in diverse
447 biological processes and stress responses (Xu et al., 2017). Previously, approximately
448 20% of the genes in rice were thought to be NATs (Li et al., 2006). In this study, we
449 found that nearly 60% of genes can be classified as NAT pairs, suggesting the superior
450 coverage of lrRNA_seq in NAT identification (Table 1). Furthermore, since some
451 NATs could be involved in multiple NAT pairs and a large number of transcript
452 isoforms was identified by lrRNA_seq, the ratio of NATs to NAT pairs is much larger
453 than 2 to 1, suggesting that in excess of 30% of the rice genome is represented by NATs.
454 Hence, our findings represent the most comprehensive study of antisense transcripts in
455 rice according to current transcriptome analyses. Given the large percentage of genes
456 that have at least one antisense sequence, several regulatory mechanisms have been
457 proposed. For example, studies in both animals and plants have suggested that NATs
458 are connected to chromatin modifications (Modarresi et al., 2012). In particular,
459 deposition of the transcriptional repressive marker H3K27me3 is a prerequisite to
460 activate expression of COOLAIR, an antisense gene of the flowering loci FLC
461 (Swiezewski et al., 2009). Additionally, siRNA generation sites have been found to be
462 clustered in overlapping genomic regions of NATs (Borsani et al., 2005; Zhang et al.,
463 2013), suggesting a role for NATs in regulating small RNA biogenesis.

464 In some studies, NATs are classified into three categories according to their
465 coding ability (Wang et al., 2014). Most NATs are considered to be non-coding loci as
466 reported by genome-wide studies in animals and plants (Katayama et al., 2005; Wang
467 et al., 2014). However, low coding potentials demonstrated by previous research,
468 largely based on prediction and examples of protein-encoding antisense genes, have
469 also been documented (Suenaga et al., 2014). Our previous proteogenomic work in

470 Arabidopsis identified 960 potential NATs with coding ability, and a majority of these
471 genes were not annotated (Zhu et al., 2017). There is no comprehensive proteomic
472 assessment on the *bona fide* coding ability of rice NATs. Here, we identified 200,830
473 proteins potentially encoded from 899,359 NATs using lrrRNA_seq-assisted
474 proteogenomics, accounting for approximately 84.5% of identified proteoforms. This
475 result suggests that these NATs do indeed have considerable coding ability in rice.

476 As described earlier in this article, pervasively transcribed NATs are able to
477 regulate gene expression via both transcriptional and post-transcriptional mechanisms
478 (Pelechano and Steinmetz, 2013). Therefore, the niche of a particular NAT pair needs
479 to be taken into account as a whole unit in functional studies. This is particularly the
480 case in the use of T-DNA or CRISPR mutants in plant functional genomics, where
481 T-DNA insertion or CRISPR editing will likely affect multiple NAT loci in close
482 vicinity to the target gene. This scenario will be further complicated when these NATs
483 contain transcript isoforms. Furthermore, some antisense transcripts may have
484 *trans*-functions in genes or gene products different from those of their sense partner
485 (Camblong et al., 2009), leading to a more complicated scenario. Thus, a
486 comprehensive pipeline for systematic characterization of NAT function should be
487 developed for both animals and plants. Bioinformatic tools are needed for functional
488 annotation and conservation evaluation of NATs among eukaryotic organisms
489 (Pelechano and Steinmetz, 2013). Importantly, the modification of specific gene
490 expression by its antisense transcripts could be developed into a potential technique as
491 our understanding of NAT regulation improves (Modarresi et al., 2012). In summary,
492 the regulatory mechanisms of NATs will likely become routine research topics in
493 future functional studies across eukaryotic organisms. Progress in this field will help
494 yield deeper understanding of gene regulation, interactions among close or overlapping
495 loci, and the evolution of the genomic arrangement and decoding process.

496

497 **The diversity of transcript isoforms expands the complexity of the regulatory**
498 **hierarchy from transcription to post-transcription**

499 The post-transcriptional mechanisms responsible for generating transcript
500 isoforms have been extensively investigated (Zhu et al., 2017; Reyes and Huber, 2018).
501 Recent advancement in this field indicates that together with AS, ATS and APA
502 co-ordinately contribute to the diversity of transcript isoforms, especially in humans
503 (de Klerk and t Hoen, 2015). Thus, comprehensive analysis including these
504 post-transcriptional (PT) events has been carried out in this study. Here, we have
505 classified these PT events into ten subtypes (Figure 5B and Supplemental Figure S4B,
506 C). Among these subtypes, six, including IR, MIR, SKIP, MKSIP, AE5', and AE3',
507 were pure AS events. Two events, namely ATS and APA, were pure
508 post-transcriptional regulations. The remaining two events, AFE and ALE, were a
509 combination of ATS/AS and APA/AS, respectively (Reyes and Huber, 2018). These
510 findings are different from examples in animal studies, where ATS and APA contribute
511 to isoform diversity more than alternative splicing (de Klerk and t Hoen, 2015; Anvar et
512 al., 2018). ATS- and APA-related events only accounted for 13% of the total PT events
513 in the rice lrrRNA_seq dataset (Supplemental Figure S4C). By contrast, intron-retention
514 events, IR and MIR, accounted for 56.5% of the total PT events, further demonstrating
515 the important function of lrrRNA_seq in modelling rice transcript diversity. SKIP and
516 MSKIP, AE5' and AE3', accounted for 16.3% and 14.1% of the total PT events,
517 respectively (Supplemental Figure S4C). However, the underlying mechanism of these
518 event types in regulating transcript diversity remains unclear.

519 Given that alternative splicing has a major contribution (>85%) to the transcript
520 diversity of the rice transcriptome, the mechanism for splice site (ss) selection was
521 further analysed. Conventionally, two types of spliceosome responsible for splice site
522 identification have been reported. One is defined as a U2-complex with canonical
523 sequences of GT (5'-ss) and AG (3'-ss), and the other is named as a U12-complex with
524 canonical sequences of AT (5'-ss) and AC (3'-ss) (Zdraviko J et al., 2005; Will and

525 Luhrmann, 2011). Previous srRNA_seq-based transcriptome studies have indicated
526 that U2-complex sequences accounted for approximately 99% of the total identified
527 splice sites, showing a high degree of conservation (Will and Luhrmann, 2011).
528 However, by using lrRNA_seq, we suggested that 91% of the total splice sites with
529 GT-AG pair sequences (Figure 5E) were possibly processed by conventional U2
530 splicing machinery, whereas the single GT and AG percentage dropped to 60% in AS
531 transcripts (Supplemental Figure S4D), indicating that alternatively spliced transcripts
532 may prefer to use non-canonical splice sites. Furthermore, two new pair sequences,
533 GC-AG and CT-AC, were found to account for 1.5% and 1.3% of the total splice sites,
534 respectively. This value is much higher than that of the minor U12 splicing complex
535 (~0.2%) in the lrRNA_seq dataset (Figure 5E), suggesting the presence of an
536 uncharacterized splicing complex or recognition mechanisms. Proteins that can
537 directly bind RNA sequences to regulate the splice site recognition process are
538 defined as splicing factors (Kalyna et al., 2006). Previous biochemical and structural
539 analysis has demonstrated that U1 and U2/U6 complexes may be responsible for the
540 selection of splice site sequences (Golovkin and Reddy, 1996; Shi, 2017). In
541 comparison to Arabidopsis (Zhu et al., 2017), rice splice sites showed less conservation
542 at both 5' and 3' positions (Supplemental Figure S4D). Subsequent evaluation of
543 splicing-related proteins suggested that rice splice components exhibit more splice
544 isoforms than do those of Arabidopsis (Supplemental Figure S5), implying that rice
545 may have a higher complexity of splicing machinery and corresponding splicing
546 mechanisms. However, the exact mechanism of this molecular process remains to be
547 further investigated in various plant developmental stages and under conditions of
548 stress.

549

550 **lrRNA_seq-based proteogenomics expand current knowledge of protein**
551 **translation and transcript classification**

552 Transcript isoforms have been profiled by either by srRNA_seq or lrRNA_seq in a
553 number of eukaryotic organisms. However, whether these isoforms can be truly
554 functional at the protein level is still under debate. Although case studies have
555 demonstrated the specific functions of transcript isoforms in animals and plants (Wang
556 et al., 2015; Hwang et al., 2018), several reports have proposed that the majority of
557 these isoforms will not be translated and will be degraded by RNA surveillance (Bitton
558 et al., 2015). Thus, the roles of these transcript isoforms have been suggested to be
559 similar to those of non-coding transcripts (Kuang et al., 2017). In addition, another
560 hypothesis has been proposed suggesting that these isoforms may function as a
561 reservoir of divergent transcripts for the evolution of new genes or
562 neo-functionalization of existing genes (Wu et al., 2011). To assess the coding ability
563 of these isoforms, we applied a proteogenomic analytical pipeline based on the
564 combined datasets from both srRNA_seq and lrRNA_seq. In total, we identified
565 191,862 peptides of 9,706 proteoforms/protein groups from 3-frame translations of
566 906,456 transcripts (Table 1 and Figure 6A). Previous results have indicated that
567 thousands of unannotated proteins can be identified using self-constructed protein
568 databases translated from srRNA_seq-assembled transcripts (Zhu et al., 2017; Chen et
569 al., 2019b). Similarly, an additional 96,822 unannotated peptides were translated from
570 unannotated coding loci (Figure 6B). These unannotated proteins will not be detected
571 using the conventional Uniprot protein database, indicating the superior power of
572 proteogenomics in unannotated protein identification. In addition, previously defined
573 lncRNA may have the ability to encode proteins or peptides (Supplemental Figure S2),
574 and a large number of splicing isoforms may not be translated. Furthermore, transcripts
575 could be translated using alternative frames or under various developmental/stress
576 conditions. Due to the limited throughput and coverage of current MS-based
577 proteomics, we estimate that a large number of proteins or peptides remain to be
578 discovered. Given the complexity of genome coding ability, we propose that caution

579 should be taken in defining non-coding transcripts. Additional criteria may be needed
580 to accurately classify coding and non-coding transcripts in the future.

581

582 **Proteogenomics facilitates decoding of eukaryotic genome**

583 Proteogenomics has long been used for omics-based comprehensive analysis in
584 eukaryotic organisms (Castellana et al., 2014; Zhang et al., 2014). Single profiling
585 techniques, such as transcriptome or proteome, will be reinforced when they are
586 integrated into one proteogenomic pipeline. For instance, pure transcriptomic data does
587 not provide direct evidence to assess the coding ability of the corresponding transcript
588 isoforms. In contrast, single proteomic identification is usually compromised of
589 incomplete information for genome annotation. Hence, integrative analysis using both
590 transcriptome and proteome data is more likely to identify dynamic variant proteins
591 encoded by transcript isoforms and unannotated proteins encoded by ATI under
592 specific conditions, providing additional insight into eukaryotic genome coding
593 abilities in response to external stimuli (Zhang et al., 2016). However, the analytical
594 pipeline requires further improvement by using emerging innovative biotechnologies.
595 For example, the high error rate of lrRNA_seq restrains further construction of 3-frame
596 protein databases. Thus, enhancement of sequencing accuracy is the basis for
597 improving whole-genome reannotation. Furthermore, using one combined library (*e.g.*,
598 0.5-10 k) instead of five separate libraries will increase the coverage of transcripts,
599 especially for sizes between the current library selection boundaries (Figure 2C).
600 Moreover, the lower quantification accuracy of lrRNA_seq and current mass
601 spectrometry-based proteomics results from their relatively low throughput and
602 coverage. Therefore, solving the problems of complex isoform quantification at both
603 transcriptional and protein levels will deeper our insights into the eukaryotic decoding
604 process. Last, but not least, in previous studies, approximately 40-50% of raw spectra
605 could be used by searching against either Uniprot or frame database (Zhu et al., 2017;
606 Chen et al., 2019b). Similarly, in this work, we used the same stringent criteria as two

607 previous works for database search. The low spectra usage in this study may be due to
608 the incompatibility of raw data generated by different MS/MS platforms and the search
609 engine ProteinPilot v5.0 developed by AB SCIEX. Subsequently, we have applied two
610 additional databases, the Uniprot protein database (downloaded on 2018-11-09, 97,832
611 entries) and the AS events library (21,015,710 entries), for protein/peptide
612 identification under the same searching criteria. Approximately 10.8% and 5.1% of the
613 total spectra were matched to the Uniprot and AS events database, respectively. It
614 appears that the spectra usage of frame database (5.9%, 310,391,750 entries) and the
615 newly prepared AS events database (5.1%) were slightly lower than the traditional
616 Uniprot database, suggesting the validity of our database search criteria for protein
617 identification. However, how to increase the percentage of spectra usage in such studies
618 remain to be elucidated.

619

620 **CONCLUSION**

621 It has been estimated that the human transcriptome contains over 80,000
622 transcripts with the potential to be translated into 250,000 proteins (de Klerk and t
623 Hoen, 2015; Reyes and Huber, 2018). In this study, lrrNA_seq-based
624 proteogenomics further expanded our knowledge of the complexity of the rice
625 genome and its coding potential (Figure 7). First, the high-density arrangement of
626 NATs in the rice genome elicits extensive undiscovered transcriptional or
627 post-transcriptional regulation mechanisms. Secondly, the interdependent
628 coordination among the three post-transcriptional mechanisms, ATS, AS, and APA,
629 increases the rice transcriptome by 26 times in the form of transcript isoforms. Thirdly,
630 taking into consideration the hypothetical proteins translated by aforementioned
631 transcript isoforms, we estimated that there is an approximately 18-fold increase in
632 the number of translated proteins compared with the 53,212 annotated loci in the rice
633 genome (Figure 7D). This estimation largely agrees with previous results using
634 srRNA_seq, but newly discovered mechanisms suggest an incredible level of

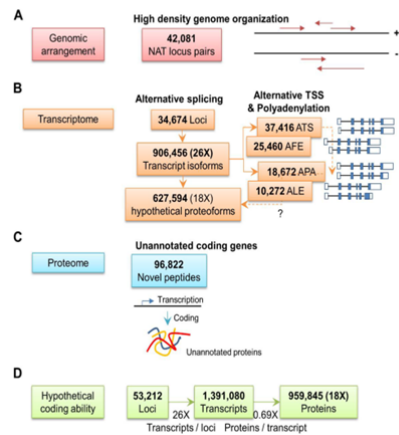


Figure 7 Modelling and estimation of genome coding ability and functional regulation, as revealed by long-read RNA-seq.

(A) Schematic showing the high-density genomic arrangement of 42,081 natural antisense transcripts (NATs). (B) Transcriptome diversity and potential coding ability. A total of 906,456 transcripts were identified from 34,674 loci by lrrNA-seq with the potential to encode 627,594 different proteoforms. In addition, thousands of alternative transcription start (ATS), alternative poly-adenylation (APA), alternative first exon (AFE), and alternative last exon (ALE) events were identified by lrrNA-seq. They may be responsible for transcript stability and translational efficiency. (C) The newly identified peptides (96,822) by proteogenomics contributes to protein diversity of eukaryotic genome. (D) An estimation of the rice genome coding ability, showing a 26-fold increase in transcript isoforms with respect to 53,212 identified loci. The estimated proteins decreased by 0.8-fold due to ATI and

1

translational redundancy. In total, a 21-fold increase from loci to protein products is estimated.

2

635 complexity in how genetic information is stored and decoded in rice genomes. The

636 unannotated loci identified in this comprehensive study also provide public
637 information for rice genome reannotation. Moreover, the integrative analytical
638 pipeline developed herein will likely serve as a valuable tool for both srRNA_seq-
639 and lrRNA_seq-based proteogenomics in eukaryotic organisms.

640

641 **MATERIALS AND METHODS**

642 **Plant materials and total RNA extraction**

643 Field-grown rice (*Oryza sativa*, Nipponbare/Geng) tissues including dry seeds,
644 14-day-old seedlings, mature plant flag leaves, stems, roots, and flowers were
645 harvested and frozen in liquid nitrogen for subsequent RNA sequencing and
646 proteomic experiments. The RNeasy Mini Kit (Qiagen, Germany) bench protocol was
647 used for plant total RNA extraction.

648

649 **Short-read RNA sequencing, data filtering, and read mapping**

650 Generally, approximately 1 µg of plant total RNA was used for library
651 construction using a TruSeq RNA Sample Prep Kit v2 (Illumina) following the
652 manufacturers' bench protocol. A strand-specific library (~250 bp) was generated
653 according to a previous description (Chen et al., 2019b). Subsequently, an Agilent
654 2100 Bioanalyzer and RT-qPCR were used to check the library quality and quantity,
655 respectively. The purified library was subjected to paired-end sequencing (2 x 101 bp)
656 using an Illumina HiSeq 4000 platform (BGI, Shenzhen, China). For subsequent
657 bioinformatic analysis, raw reads from all samples were assessed by quality control
658 steps to obtain clean reads (Supplemental Table S1). The rice reference genome
659 annotation file (Osativa_323_v7.0.gene_exons.gff3) was downloaded from Phytozome
660 (<https://phytozome.jgi.doe.gov/pz/portal.html>). The mapping and assembly pipeline
661 used was similar to that previously described for srRNA_seq (Zhu et al., 2017). The
662 assembled transcripts were used for subsequent specialized transcript characterization.

663

664 **Single-molecule long-read RNA sequencing and data analysis**

665 The library construction steps and sequencing strategies were described
666 previously (Zhu et al., 2017) and performed with minor modifications (Supplemental
667 Table S2). In general, five libraries (*i.e.*, 0.5-1 k, 1-2 k, 2-3 k, 3-6 k, and 5-10 k) were
668 generated and sequenced using 16 SMRT cells for each tissue type on a Pacific
669 Biosciences (CA, USA) RSII platform (BGI). The resulting raw data were processed
670 by the ToFu pipeline as described on the company website
671 ([https://github.com/PacificBiosciences/
672 cDNA_primer/wiki/tofu-Tutorial-\(optional\).-Removing-redundant-transcripts](https://github.com/PacificBiosciences/cDNA_primer/wiki/tofu-Tutorial-(optional).-Removing-redundant-transcripts)). Both
673 high- and low-quality full-length transcripts were subjected to base correction by two
674 rounds of BLAST against the Phytozome reference genome and cDNA sequences for
675 subsequent bioinformatic analysis.

676

677 **Transcript re-mapping and identification of alternative splicing**

678 The soft-masked rice genome sequences were downloaded from Phytozome
679 v12.1.6 (<https://phytozome.jgi.doe.gov/pz/portal.html>; last accessed on May 3, 2018)
680 and indexed using gmap_build (version 2018-03-25). Re-mapping of the previously
681 genome-guided assembled transcripts (total 120,958) from Illumina stranded
682 paired-end reads (srRNA_seq dataset) and Pacbio full-length transcripts (total
683 1,100,036) from the lrRNA_seq dataset to the rice genome was performed using
684 GMAP (Abdel-Ghany et al., 2016) with the following parameters: --no-chimaeras
685 --cross-species --min-identity 0.98 --allow-close-indels 2 -n 1 -z sense_force, where
686 only the transcripts aligned with a minimum identity of 0.98 and correct strand
687 information were included for subsequent analyses.

688 Further filtering was performed by comparison to the extant rice gene models,
689 retaining transcripts that contained at least one correct junction or covered an intact
690 exon. Then, AS events were analysed using ASprofile
691 (<https://ccb.jhu.edu/software/ASprofile/>) according to a previous description (Zhu et

692 al., 2017). A CIRCOS diagram was drafted using the AS frequency mapped on the
693 rice genome with a 300-kb sliding window. Additionally, the splice site statistics and
694 conservation analysis were summarized and constructed using the online software
695 WebLogo v3 (<http://weblogo.threeplusone.com/>) (Crooks et al., 2004). Splicing
696 variants were identified by using full-length transcripts after two rounds of correction
697 against the Nipponbare reference genome and cDNAs as described previously (Reyes
698 and Huber, 2018). Redundant transcripts were then removed based on BLAST results
699 filtered by parameters as 98% identity and >3 mismatches. In addition, unannotated
700 transcripts of sr_RNA seq and lr_RNA seq datasets were identified by performing
701 comparisons using the same criteria against the Phytozome annotation of rice
702 transcripts. After the removal of redundancy, the remaining transcripts was
703 characterized as ‘unannotated transcripts’ (Supplemental Table S8).

704

705 **Characterization of natural antisense, fusion and intergenic transcripts**

706 Natural antisense transcripts (NATs) were identified according to previous
707 methods with minor modifications (Wang et al., 2014; Xu et al., 2017). In general,
708 transcripts located in different strands of genomic DNA with overlapping coordinates
709 were used for NATs characterization.

710 Fusion transcripts were analysed using previously described procedures with
711 minor modifications (Weirather et al., 2015; Wang et al., 2016). In detail, transcripts
712 mapped to two or more places on the rice genome were selected for further analysis.

713 Intergenic transcripts were identified by choosing transcripts mapped to
714 intergenic regions (class u transcripts by GMAP).

715

716 **Gene ontology and pathway enrichment**

717 Generally, gene ontology (GO) functional enrichment was conducted using the
718 AgriGOv2 annotation database ([http://systemsbiology.cau.edu.cn/agriGOv2/
719 download.php](http://systemsbiology.cau.edu.cn/agriGOv2/download.php)). Kyoto Encyclopedia of Genes and Genomes (KEGG) pathway

720 enrichment analysis was carried out according to the KOBAS database
721 (<http://kobas.cbi.pku.edu.cn>). Significant GO and KEGG terms were identified using
722 the following parameters: gene number (> 5) and adjusted *P* value (< 0.05).

723

724 **Plant protein extraction, processing and MS/MS analysis.**

725 Plant total proteins were extracted according to a previous description (Chen et al.,
726 2014; Zhu et al., 2018; Chen et al., 2019a) for proteomic identification. In general,
727 approximately 10 g rice tissue samples were ground in liquid nitrogen for total protein
728 extraction. Trypsin or Glu-C digestion was performed on two parallel batches of the
729 samples. The resulting peptides were separated and detected using Q Exactive tandem
730 mass spectrometer equipped with an Orbitrap analyzer (Thermo Scientific). In brief,
731 mixed peptides were subsequently fractionated by using a C₁₈-Gemini column (4.6 mm
732 × 250 mm, 5 μm particle size) on the Shimadzu LC-20AB system (Shimadzu, China).
733 An elution gradient of ~60 min was used for peptide separation with 5% (v/v)
734 acetonitrile (pH 9.8) as mobile phase A and 95% (v/v) acetonitrile (pH 9.8) as mobile
735 phase B. The gradient elution profile was composed of 5% mobile phase B for 10 min,
736 5-35% mobile phase B for 40 min, 35-95% mobile phase B for 1 min, then maintained
737 at 100% mobile phase B for 3 min and ending with 5% mobile phase B for 10 min. The
738 flow rate was adjusted to 1 mL/min and UV absorbance (214nm) was monitored. A
739 total of 20 fractions were collected and then freeze-dried *via* speed-vacuum method.
740 LC-MS/MS detection was carried out on a Q-Exactive mass spectrometer (Thermo
741 Fisher Scientific, San Jose, CA) equipped with a nanoESI source. Generally,
742 fractionated peptides were first loaded onto a trap column and then eluted into a
743 self-packed C₁₈ analytical column (3 μm particle size, 75 μm × 150 mm). A constant
744 flow rate was set at 300 nL/min and mobile phase B (0.1% [v/v] formic acid and 98%
745 [v/v] acetonitrile) was used to establish a 65 min gradient, which consisted of 5% B
746 during 0-8 min, 8-35% B during 8-43 min, 35-60% B during 43-48 min, 60-80% B
747 during 48-50 min, 80% B during 50-55 min and a final step in 5% B during 55-65 min.

748 MS scans were carried out using the data-dependent acquisition mode with the
749 following parameters: the ion source voltage was set to 1.6 kV; each scan cycle
750 consisted of one full-scan mass spectrum (with m/z ranging from 350 to 1600 m/z and
751 charge states from 2 to 7) followed by 20 MS/MS events (with m/z starting from 100
752 m/z); the resolutions of MS and MS/MS were set to 70000 and 17500, respectively; the
753 threshold count was set to 10000 to activate MS/MS accumulation and former target
754 ion exclusion was set for 15 s; HCD collision energy was set to 27; AGCs of MS and
755 MS/MS were set to 3E6 and 1E6, respectively.

756 In addition to the 24 datasets from the PRIDE database (Supplemental Table S7),
757 7,368,042 high-quality raw spectra were used for subsequent proteogenomic analysis
758 (Figure 6A). All raw spectral data were processed using the same quality parameters.
759

760 **Database construction and mass spectrometry dataset searching.**

761 A self-constructed virtual peptide library (155,195,875 entries) was generated
762 based on previously developed protocols with minor modifications. Briefly,
763 three-frame translations of strand-specific transcripts from both srRNA_seq and
764 lrRNA_seq were performed. Redundant peptide sequences were removed, and the
765 sequences were combined. Peptide entries longer than 6 amino acids were filtered for
766 inclusion in the final virtual library. In total, peptides generated from 1,221,140
767 transcripts containing 6-10 amino acids (52,664,121 entries), 11-80 amino acids
768 (96,670,677 entries), and more than 80 amino acids (5,861,077 entries) were used for
769 subsequent protein identification. The AS events library (21,015,710 entries) was
770 generated as described previously (Zhu et al., 2017). In general, the strand-specific
771 cDNA sequences of identified PT events and their junctions underwent 3-frame
772 translation to generate target entries in this library. The database search was carried
773 out according to a previous description (Chen et al., 2014). Briefly, ProteinPilot
774 software (v5.0, AB SCIEX) was used for peptide and protein identification with
775 global $FDR < 0.01$. Proteoforms/Protein groups with at least two unique peptides at

776 the 95% confidence level were summarized as conservative/minimum number of
777 proteoforms for further proteogenomic analysis (Supplemental Table S9).

778

779 **Reverse transcription quantitative PCR (RT-qPCR) validation of select**
780 **transcripts**

781 Approximately 5 µg total RNA from rice was extracted and reverse-transcribed
782 into cDNA following the bench protocol of Superscript First-Strand Synthesis System
783 (Invitrogen, USA). RT-qPCR was carried out following previous experimental
784 description (Zhu et al., 2017). Transcript-specific primers used in RT-qPCR were
785 summarized in Supplemental Table S10.

786

787 **Accession numbers**

788 The data from srRNA_seq and lrRNA_seq has been uploaded to the Sequence
789 Read Archive (<https://www.ncbi.nlm.nih.gov/sra>) under Bioproject PRJNA482217.
790 We have submitted our proteomic raw data into the PRoteomics IDentifications
791 (PRIDE) database with accession number PXD013462.

792

793 **Supplemental data**

794 The following supplemental materials are available.

795 **Supplemental Figure S1.** Characterization and comparison of fusion transcripts
796 between srRNA_seq and lrRNA_seq.

797 **Supplemental Figure S2.** Identification of intergenic transcripts and lncRNA.

798 **Supplemental Figure S3.** Statistics and functional analysis of NATs.

799 **Supplemental Figure S4.** Comparison of post-transcriptional events and single splice
800 site analysis between srRNA_seq and lrRNA_seq.

801 **Supplemental Figure S5.** Comparison of rice and Arabidopsis splicing factor
802 transcript isoforms.

803 **Supplemental Table S1.** Basic sequencing information for srRNA_seq.

804 **Supplemental Table S2.** Basic sequencing information for lrRNA_seq.
805 **Supplemental Table S3.** GO enrichment of fusion transcripts identified by
806 lrRNA_seq.
807 **Supplemental Table S4.** GO enrichment of natural antisense transcripts identified by
808 lrRNA_seq.
809 **Supplemental Table S5.** Functional annotation of natural antisense transcripts
810 identified by lrRNA_seq.
811 **Supplemental Table S6.** Identification and annotation of ATS and APA.
812 **Supplemental Table S7.** List of protein datasets used for protein database search.
813 **Supplemental Table S8.** Annotation file of unannotated transcripts identified from
814 lrRNA_seq dataset.
815 **Supplemental Table S9.** List of identified proteoforms/protein groups and their
816 supporting information.
817 **Supplemental Table S10.** Primers used in this study.

818

819 **ACKNOWLEDGEMENTS**

820 This work was supported by the Funds of Shandong “Double Top” Program, the
821 National Natural Science Foundation of China (NSFC81401561 and 91535109), the
822 Shenzhen Virtual University Park Support Scheme to CUHK Shenzhen Research
823 Institute (YFJGJS1.0), the Natural Science Foundation of Hunan Province
824 (2019JJ50263) and the Hong Kong Research Grant Council (AoE/M-05/12,
825 AoE/M-403/16, GRF14160516, 14177617, 12100318).

826

827

828

829 **Table 1**

Table 1 Comparison of existing database with short-read RNA sequencing and long-read RNA sequencing

Type	MSU_Osv7	srRNA seq	lrRNA seq	Fold
------	----------	-----------	-----------	------

Traditional gene models

Number of loci	42,189	15,451	34,674	2.24
Number of mapped transcripts	52,424	120,950	906,456	7.49
Novel loci	0	5,686	11,023	1.94
Novel transcript	0	65,723	102,614	1.56
Unmapped transcripts	0	8	193,580	
Number of transcripts (Total)	52,424	120,958	1,100,036	9.09
Loci with splicing variants	6,384	13,745	32,780	2.38
Total splicing isoforms	6,384	104,942	867,136	8.26
MSU loci with splicing variants	6,384	6,540	20,142	3.08
MSU splicing variants	16,617	52,102	801,194	15.38
Novel loci with splicing variants		7,205	7,505	
Novel splicing variants		52,840	65,942	

Specialized transcripts

Natural antisense transcripts	21,759	78,833	899,359	11.41
Fusion transcripts	0	1,192	7,804	6.55
Intergenic transcripts	0	28,422	31,095	1.09

830

831

832 FIGURE LEGENDS

833 **Figure 1. Schematic view of the experimental and analytical pipeline used in this**

834 **study.** srRNA_seq and lrRNA_seq was performed by using Hiseq 4000 and Pacbio

835 RSII platform. Proteomic analysis was performed by using Q Exactive platform. Data

836 mining was carried out by using online deposited datasets. Major steps of analytical

837 pipeline are shown.

838

839 **Figure 2. Comparison of transcript properties between srRNA_seq and**

840 **lrRNA_seq.**

841 (A) Circos diagram of specialized transcripts identified by srRNA_seq and lrRNA_seq.

842 1, total transcripts identified by srRNA_seq; 2, total transcript identified by

843 lrRNA_seq; 3, intergenic transcripts identified by srRNA_seq; 4, intergenic transcripts

844 identified by lrRNA_seq; 5, NATs identified by srRNA_seq; 6, NATs identified by

845 lrRNA_seq; 7, fusion transcripts identified by srRNA_seq; 8, fusion transcripts

846 identified by lrRNA_seq. (B) Boxplot of transcript lengths summarized in the three
847 datasets using MSU_Osv7 annotation, srRNA_seq and lrRNA_seq. Histogram plots
848 showing the frequency of transcript lengths between (C) srRNA_seq and (D)
849 lrRNA_seq.

850

851 **Figure 3. Comparative analysis of fusion transcripts.**

852 (A) Venn diagram showing the overlapping and unique fusion transcripts identified by
853 srRNA_seq and lrRNA_seq. (B) Summary of fusion transcript subtypes. (C) Circos
854 representation of fusion transcripts consisting of two genes. (D) Venn diagram
855 presenting the overlapping and unique genes involved in fusion transcript formation.
856 (E) GO and KEGG enrichment analysis of fusion genes. (F) Loci frequency present in
857 fusion transcripts. (G) RT-PCR validation of fusion transcripts. M, marker; bp, base
858 pair; F1, F2, F3, three fusion transcripts.

859

860 **Figure 4 Comparison of natural antisense transcripts identified by srRNA_seq**

861 **and lrRNA_seq.** (A) Venn diagram showing the overlapped and unique transcripts
862 present in the current annotation in comparison to the srRNA_seq and lrRNA_seq
863 datasets. (B) Classification of 5 subtypes of NATs. (C) Summary of NATs identified by
864 lrRNA_seq at the levels of exon/intron pairs, transcript pairs and locus pairs. (D)
865 Summary of NAT subtypes in two strands of genomic DNA. (E, F) GO and KEGG
866 enrichment analysis of NATs. (G) RT-PCR validation of antisense transcripts. M,
867 marker; bp, base pair; A1-A5, antisense transcripts.

868

869

870

871 **Figure 5. Identification of alternative transcription starts, alternative splicing,**
872 **and alternative polyadenylation.**

873 (A) Violin plot of splicing variants identified in MSU_Osv7 annotation, srRNA_seq,
874 and lrRNA_seq. (B) Circos representation of post-transcriptional events identified in
875 srRNA_seq, and lrRNA_seq. *, density of transcripts recorded in MSU_Os7
876 annotation; 1, intron retention (IR); 2, multiple intron retention (MIR); 3, exon skipping
877 (SKIP); 4, multiple exon skipping (MSKIP); 5, alternative exon 5' (AE5'); 6,
878 alternative exon 3' (AE3'); 7, alternative transcript start (ATS); 8, alternative
879 polyadenylation (APA); 9, alternative first exon (AFE); and 10, alternative last exon
880 (ALE). Exon comparisons (C), paired splicing sites comparisons (D), and statistical
881 analysis of paired splicing sites (E) among MSU_Os7 annotation, srRNA_seq and
882 lrRNA_seq. (F) Summary of identified PT events and peptides in srRNA_seq and
883 lrRNA_seq.

884

885 **Figure 6. Assessment of coding potential by proteogenomics.**

886 (A) Basic parameters used in proteomic database search. (B) Summary of known and
887 unannotated peptides. (C) Distribution of identified proteoforms/protein groups and
888 peptides.

889

890 **Figure 7. Modelling and estimation of genome coding ability and functional**
891 **regulation, as revealed by long-read RNA_seq.**

892 (A) Schematic showing the high-density genomic arrangement of 42,081 natural
893 antisense transcripts (NATs). (B) Transcriptome diversity and potential coding ability.
894 A total of 90,6456 transcripts were identified from 34,674 loci by lrRNA_seq with the
895 potential to encode 627,594 different proteoforms. In addition, thousands of alternative
896 transcription start (ATS), alternative poly-adenylation (APA), alternative first exon
897 (AFE), and alternative last exon (ALE) events were identified by lrRNA_seq. They
898 may be responsible for transcript stability and translational efficiency. (C) The newly
899 identified peptides (96,822) by proteogenomics contributes to protein diversity of
900 eukaryotic genome. (D) An estimation of the rice genome coding ability, showing a

901 26-fold increase in transcript isoforms with respect to 53,212 identified loci. The
902 estimated proteins decreased by 0.8-fold due to ATI and translational redundancy. In
903 total, a 21-fold increase from loci to protein products is estimated.

904

905

Parsed Citations

Abdel-Ghany SE, Hamilton M, Jacobi JL, Ngam P, Devitt N, Schilkey F, Ben-Hur A, Reddy AS (2016) A survey of the sorghum transcriptome using single-molecule long reads. Nat Commun 7: 11706

Pubmed: [Author and Title](#)

Google Scholar: [Author Only Title Only Author and Title](#)

Anvar SY, Allard G, Tseng E, Sheynkman GM, De EK, Vermaat M, Yin RH, Johansson HE, Ariyurek Y, Den JD, et al (2018) Full-length mRNA sequencing uncovers a widespread coupling between transcription initiation and mRNA processing. Genome Biol 19: 46

Pubmed: [Author and Title](#)

Google Scholar: [Author Only Title Only Author and Title](#)

Balbin O, Malik R, Dhanasekaran S, Prensner J, Cao X, Wu Y, Robinson D, Wang R, Chen G, Beer D, et al (2015) The landscape of antisense gene expression in human cancers. Genome Res 25: 1068-1079

Pubmed: [Author and Title](#)

Google Scholar: [Author Only Title Only Author and Title](#)

Bitton D, Atkinson S, Rallis C, Smith G, Ellis D, Chen Y, Malecki M, Codlin S, Lemay J, Cotobal C, et al (2015) Widespread exon skipping triggers degradation by nuclear RNA surveillance in fission yeast. Genome Res 25: 884-896

Pubmed: [Author and Title](#)

Google Scholar: [Author Only Title Only Author and Title](#)

Borsani O, Zhu J, Verslues PE, Sunkar R, Zhu JK (2005) Endogenous siRNAs derived from a pair of natural cis-antisense transcripts regulate salt tolerance in Arabidopsis. Cell 123: 1279-1291

Pubmed: [Author and Title](#)

Google Scholar: [Author Only Title Only Author and Title](#)

Bouthier dITC, Blanchard L, Dulermo R, Ludanyi M, Devigne A, Armengaud J, Sommer S, De GA (2015) The abundant and essential HU proteins in Deinococcus deserti and Deinococcus radiodurans are translated from leaderless mRNA. Microbiology 161: 2410-2422

Pubmed: [Author and Title](#)

Google Scholar: [Author Only Title Only Author and Title](#)

Bøvre K, Szybalski W (1969) Patterns of convergent and overlapping transcription within the b2 region of coliphage λ. Virology 38: 614-626

Pubmed: [Author and Title](#)

Google Scholar: [Author Only Title Only Author and Title](#)

Camblong J, Beyrouthy N, Guffanti E, Schlaepfer G, Steinmetz LM, Stutz F (2009) Trans-acting antisense RNAs mediate transcriptional gene cosuppression in S. cerevisiae. Genes Dev 23: 1534-1545

Pubmed: [Author and Title](#)

Google Scholar: [Author Only Title Only Author and Title](#)

Castellana NE, Payne SH, Shen Z, Stanke M, Bafna V, Briggs SP (2008) Discovery and revision of Arabidopsis genes by proteogenomics. Proc Natl Acad Sci USA 105: 21034-21038

Pubmed: [Author and Title](#)

Google Scholar: [Author Only Title Only Author and Title](#)

Castellana NE, Shen Z, He Y, Walley JW, Cassidy CJ, Briggs SP, Bafna V (2014) An automated proteogenomic method uses mass spectrometry to reveal novel genes in Zea mays. Mol Cell Proteomics 13: 157-167

Pubmed: [Author and Title](#)

Google Scholar: [Author Only Title Only Author and Title](#)

Chang CY, Lin WD, Tu SL (2014) Genome-wide analysis of heat-sensitive alternative splicing in Physcomitrella patens. Plant Physiol 165: 826-840

Pubmed: [Author and Title](#)

Google Scholar: [Author Only Title Only Author and Title](#)

Chapman B, Bellgard M (2017) Plant proteogenomics: Improvements to the grapevine genome annotation. Proteomics 17: 1700197

Pubmed: [Author and Title](#)

Google Scholar: [Author Only Title Only Author and Title](#)

Chen MX, Sun C, Zhang KL, Song YC, Tian Y, Chen X, Liu YG, Ye NH, Zhang J, Qu S, Zhu FY (2019a) SWATH-MS-facilitated proteomic profiling of fruit skin between Fuji apple and a red skin bud sport mutant. BMC Plant Biology 19: 1-13

Pubmed: [Author and Title](#)

Google Scholar: [Author Only Title Only Author and Title](#)

Chen MX, Zhu FY, Wang FZ, Ye NH, Gao B, Chen X, Zhao SS, Fan T, Cao YY, Liu TY, et al (2019b) Alternative splicing and translation play important roles in hypoxic germination in rice. J Exp Bot 70: 817-833

Pubmed: [Author and Title](#)

Google Scholar: [Author Only Title Only Author and Title](#)

Chen X, Chan WL, Zhu FY, Lo C (2014) Phosphoproteomic analysis of the non-seed vascular plant model Selaginella moellendorffii. Proteome Sci 12: 16

Pubmed: [Author and Title](#)

Google Scholar: [Author Only](#) [Title Only](#) [Author and Title](#)

Conesa A, Madrigal P, Tarazona S, Gomezcabrero D, Cervera A, Mcpherson A, Szcześniak MW, Gaffney DJ, Elo LL, Zhang X, et al (2016) A survey of best practices for RNA-seq data analysis. Genome Biol 17: 13

Pubmed: [Author and Title](#)

Google Scholar: [Author Only](#) [Title Only](#) [Author and Title](#)

Crooks GE, Hon G, Chandonia JM, Brenner SE (2004) WebLogo: a sequence logo generator. Genome Res 14: 1188-1190

Pubmed: [Author and Title](#)

Google Scholar: [Author Only](#) [Title Only](#) [Author and Title](#)

De Groot A, Roche D, Fernandez B, Ludanyi M, Cruveiller S, Pignol D, Vallenet D, Armengaud J, Blanchard L (2014) RNA sequencing and proteogenomics reveal the importance of leaderless mRNAs in the radiation-tolerant bacterium *Deinococcus deserti*. Genome Biol Evol 6: 932-948

Pubmed: [Author and Title](#)

Google Scholar: [Author Only](#) [Title Only](#) [Author and Title](#)

de Klerk E, t Hoen PA (2015) Alternative mRNA transcription, processing, and translation: insights from RNA sequencing. Trends Genet 31: 128-139

Pubmed: [Author and Title](#)

Google Scholar: [Author Only](#) [Title Only](#) [Author and Title](#)

Deveson IW, Brunck ME, Blackburn J, Tseng E, Hon T, Clark TA, Clark MB, Crawford J, Dinger ME, Nielsen LK, et al (2018) Universal alternative splicing of noncoding exons. Cell Syst 6: 245-255

Pubmed: [Author and Title](#)

Google Scholar: [Author Only](#) [Title Only](#) [Author and Title](#)

Duan L, Xiao W, Xia F, Liu H, Xiao J, Li X, Wang S (2016) Two different transcripts of a LAMMER kinase gene play opposite roles in disease resistance. Plant Physiol 172: 1959-1972

Pubmed: [Author and Title](#)

Google Scholar: [Author Only](#) [Title Only](#) [Author and Title](#)

Eckardt NA (2013) The plant cell reviews alternative splicing. Plant Cell 25: 3639

Pubmed: [Author and Title](#)

Google Scholar: [Author Only](#) [Title Only](#) [Author and Title](#)

Edwards PA (2010) Fusion genes and chromosome translocations in the common epithelial cancers. J Pathol 220: 244-254

Pubmed: [Author and Title](#)

Google Scholar: [Author Only](#) [Title Only](#) [Author and Title](#)

Edwards PA, Howarth KD (2012) Are breast cancers driven by fusion genes? Breast Cancer Res 14: 303

Faghihi MA, Wahlestedt C (2009) Regulatory roles of natural antisense transcripts. Nat Rev Mol Cell Biol 10: 637-643

Pubmed: [Author and Title](#)

Google Scholar: [Author Only](#) [Title Only](#) [Author and Title](#)

Golovkin M, Reddy AS (1996) Structure and expression of a plant U1 snRNP 70K gene: alternative splicing of U1 snRNP 70K pre-mRNAs produces two different transcripts. Plant Cell 8: 1421-1435

Pubmed: [Author and Title](#)

Google Scholar: [Author Only](#) [Title Only](#) [Author and Title](#)

Hwang I, Cao D, Na Y, Kim DY, Zhang T, Yao J, Oh H, Hu J, Zheng H, Yao Y, et al (2018) Far Upstream Element-Binding Protein 1 Regulates LSD1 Alternative Splicing to Promote Terminal Differentiation of Neural Progenitors. Stem Cell Rep 10: 1208-1221

Pubmed: [Author and Title](#)

Google Scholar: [Author Only](#) [Title Only](#) [Author and Title](#)

Ingolia NT, Lareau LF, Weissman JS (2011) Ribosome profiling of mouse embryonic stem cells reveals the complexity and dynamics of mammalian proteomes. Cell 147: 789-802

Pubmed: [Author and Title](#)

Google Scholar: [Author Only](#) [Title Only](#) [Author and Title](#)

Jaffe JD, Berg HC, Church GM (2004) Proteogenomic mapping as a complementary method to perform genome annotation. Proteomics 4: 59-77

Pubmed: [Author and Title](#)

Google Scholar: [Author Only](#) [Title Only](#) [Author and Title](#)

Jensen TH, Jacquier A, Libri D (2013) Dealing with pervasive transcription. Mol Cell 52: 473-484

Pubmed: [Author and Title](#)

Google Scholar: [Author Only](#) [Title Only](#) [Author and Title](#)

Kalsotra A, Cooper TA (2011) Functional consequences of developmentally regulated alternative splicing. Nat Rev Genet 12: 715-729

Pubmed: [Author and Title](#)

Google Scholar: [Author Only](#) [Title Only](#) [Author and Title](#)

Kalyna M, Lopato S, Voronin V, Barta A (2006) Evolutionary conservation and regulation of particular alternative splicing events in

plant SR proteins. Nucleic Acids Res 34: 4395-4405

Pubmed: [Author and Title](#)

Google Scholar: [Author Only Title Only Author and Title](#)

Katayama S, Tomaru Y, Kasukawa T, Waki K, Nakanishi M, Nakamura M, Nishida H, Yap CC, Suzuki M, Kawai J, et al (2005) Antisense transcription in the mammalian transcriptome. Science 309: 1564-1566

Pubmed: [Author and Title](#)

Google Scholar: [Author Only Title Only Author and Title](#)

Kuang Z, Boeke J, Canzar S (2017) The dynamic landscape of fission yeast meiosis alternative-splice isoforms. Genome Res 27: 145-156

Pubmed: [Author and Title](#)

Google Scholar: [Author Only Title Only Author and Title](#)

Kucharova V, Wiker HG (2015) Proteogenomics in microbiology: Taking the right turn at the junction of genomics and proteomics. Proteomics 14: 2360-2675

Pubmed: [Author and Title](#)

Google Scholar: [Author Only Title Only Author and Title](#)

Kumar D, Mondal AK, Kutum R, Dash D (2016) Proteogenomics of rare taxonomic phyla: A prospective treasure trove of protein coding genes. Proteomics 16: 226-240

Pubmed: [Author and Title](#)

Google Scholar: [Author Only Title Only Author and Title](#)

Laloum T, Martin G, Duque P (2018) Alternative Splicing Control of Abiotic Stress Responses. Trends Plant Sci 23: 140-150

Pubmed: [Author and Title](#)

Google Scholar: [Author Only Title Only Author and Title](#)

Li L, Wang X, Stolc V, Li X, Zhang D, Su N, Tongprasit W, Li S, Cheng Z, Wang J, et al (2006) Genome-wide transcription analyses in rice using tiling microarrays. Nat Genet 38: 124-129

Pubmed: [Author and Title](#)

Google Scholar: [Author Only Title Only Author and Title](#)

Locardpaulet M, Pible O, Peredo AGD, Alhabazin B, Almunia C, Burltschiltz O, Armengaud J (2015) Clinical implications of recent advances in proteogenomics. Expert Rev of Proteomic 13: 185-199

Pubmed: [Author and Title](#)

Google Scholar: [Author Only Title Only Author and Title](#)

Lomsadze A, Gemayel K, Tang S, Borodovsky M (2018) Modeling leaderless transcription and atypical genes results in more accurate gene prediction in prokaryotes. Genome Res 28: 1079-1089

Pubmed: [Author and Title](#)

Google Scholar: [Author Only Title Only Author and Title](#)

McManus CJ, Duff MO, Eipper-Mains J, Graveley BR (2010) Global analysis of trans-splicing in Drosophila. Proc Natl Acad Sci USA 107: 12975-12979

Pubmed: [Author and Title](#)

Google Scholar: [Author Only Title Only Author and Title](#)

Meier F, Geyer PE, Winter SV, Cox J, Mann M (2018) BoxCar acquisition method enables single-shot proteomics at a depth of 10,000 proteins in 100 minutes. Nature methods 15: 440-44

Pubmed: [Author and Title](#)

Google Scholar: [Author Only Title Only Author and Title](#)

Menschaert G, Van Criekeing W, Notelaers T, Koch A, Crappe J, Gevaert K, Van Damme P (2013) Deep proteome coverage based on ribosome profiling aids mass spectrometry-based protein and peptide discovery and provides evidence of alternative translation products and near-cognate translation initiation events. Mol Cell Proteomics 12: 1780-1790

Pubmed: [Author and Title](#)

Google Scholar: [Author Only Title Only Author and Title](#)

Mills JD, Chen BJ, Ueberham U, Arendt T, Janitz M (2016) The antisense transcriptome and the human brain. J Mol Neurosci 58: 1-15

Pubmed: [Author and Title](#)

Google Scholar: [Author Only Title Only Author and Title](#)

Modarresi F, Faghihi MA, Lopez-Toledano MA, Fatemi RP, Magistri M, Brothers SP, van der Brug MP, Wahlestedt C (2012) Inhibition of natural antisense transcripts in vivo results in gene-specific transcriptional upregulation. Nat Biotechnol 30: 453-459

Pubmed: [Author and Title](#)

Google Scholar: [Author Only Title Only Author and Title](#)

Morrissy AS, Griffith M, Marra MA (2011) Extensive relationship between antisense transcription and alternative splicing in the human genome. Genome Res 21: 1203-1212

Pubmed: [Author and Title](#)

Google Scholar: [Author Only Title Only Author and Title](#)

Mourier T, Jeffares DC (2003) Eukaryotic intron loss. Science 300: 1393

Pubmed: [Author and Title](#)

Downloaded from on February 28, 2020 - Published by www.plantphysiol.org
Copyright © 2019 American Society of Plant Biologists. All rights reserved.

- Google Scholar: [Author Only](#) [Title Only](#) [Author and Title](#)
- Nesvizhskii AI (2014) Proteogenomics: concepts, applications and computational strategies. Nature methods 11: 1114-1125**
Pubmed: [Author and Title](#)
Google Scholar: [Author Only](#) [Title Only](#) [Author and Title](#)
- Okonechnikov K, Imai-Matsushima A, Paul L, Seitz A, Meyer TF, Garcia-Alcalde F (2016) InFusion: Advancing discovery of fusion genes and chimeric transcripts from deep RNA-sequencing data. PLoS One 11: e0167417**
Pubmed: [Author and Title](#)
Google Scholar: [Author Only](#) [Title Only](#) [Author and Title](#)
- Ouyang S, Zhu W, Hamilton J, Lin H, Campbell M, Childs K, Thibaud-Nissen F, Malek RL, Lee Y, Zheng L, et al (2007) The TIGR rice genome annotation resource: improvements and new features. Nucleic Acids Res 35: D883-887**
Pubmed: [Author and Title](#)
Google Scholar: [Author Only](#) [Title Only](#) [Author and Title](#)
- Pan Q, Shai O, Lee L, Frey B, Blencowe B (2008) Deep surveying of alternative splicing complexity in the human transcriptome by high-throughput sequencing. Nat Genet 40: 1413-1415**
Pubmed: [Author and Title](#)
Google Scholar: [Author Only](#) [Title Only](#) [Author and Title](#)
- Pelechano V, Steinmetz L (2013) Gene regulation by antisense transcription. Nat Rev Genet 14: 880**
Pubmed: [Author and Title](#)
Google Scholar: [Author Only](#) [Title Only](#) [Author and Title](#)
- Prescott EM, Proudfoot NJ (2002) Transcriptional collision between convergent genes in budding yeast. Proc Natl Acad Sci USA 99: 8796-8801**
Pubmed: [Author and Title](#)
Google Scholar: [Author Only](#) [Title Only](#) [Author and Title](#)
- Reddy AS, Marquez Y, Kalyna M, Barta A (2013) Complexity of the alternative splicing landscape in plants. Plant Cell 25: 3657-3683**
Pubmed: [Author and Title](#)
Google Scholar: [Author Only](#) [Title Only](#) [Author and Title](#)
- Ren Z, Qi D, P Nina, L Kai, Wen B, Zhou R, Xu S, Liu S, Jones AR (2019) Improvements to the rice genome annotation through large-scale analysis of RNA-seq and proteomics data sets. Mol Cell Proteomics 18: 86-98**
Pubmed: [Author and Title](#)
Google Scholar: [Author Only](#) [Title Only](#) [Author and Title](#)
- Reyes A, Huber W (2018) Alternative start and termination sites of transcription drive most transcript isoform differences across human tissues. Nucleic Acids Res 46: 582-592**
Pubmed: [Author and Title](#)
Google Scholar: [Author Only](#) [Title Only](#) [Author and Title](#)
- Ruhl C, Stauffer E, Kahles A, Wagner G, Drechsel G, Ratsch G, Wachter A (2012) Polypyrimidine tract binding protein homologs from Arabidopsis are key regulators of alternative splicing with implications in fundamental developmental processes. Plant Cell 24: 4360-4375**
Pubmed: [Author and Title](#)
Google Scholar: [Author Only](#) [Title Only](#) [Author and Title](#)
- Sharon D, Tilgner H, Grubert F, Snyder M (2013) A single-molecule long-read survey of the human transcriptome. Nat Biotechnol 31: 1009-1014**
Pubmed: [Author and Title](#)
Google Scholar: [Author Only](#) [Title Only](#) [Author and Title](#)
- Shi YG (2017) Mechanistic insights into precursor messenger RNA splicing by the spliceosome. Nat Rev Mol Cell Bio 18: 655-670**
Pubmed: [Author and Title](#)
Google Scholar: [Author Only](#) [Title Only](#) [Author and Title](#)
- Sonenberg N, Hinnebusch AG (2009) Regulation of translation initiation in eukaryotes: mechanisms and biological targets. Cell 136: 731-745**
Pubmed: [Author and Title](#)
Google Scholar: [Author Only](#) [Title Only](#) [Author and Title](#)
- Steijger T, Abril JF, Engström PG, Kokocinski F, Hubbard TJ, Guigó R, Harrow J, Bertone P (2013) Assessment of transcript reconstruction methods for RNA-seq. Nat Methods 10: 1177**
Pubmed: [Author and Title](#)
Google Scholar: [Author Only](#) [Title Only](#) [Author and Title](#)
- Su WY, Li JT, Cui Y, Hong J, Du W, Wang YC, Lin YW, Xiong H, Wang JL, Kong X, et al (2012) Bidirectional regulation between WDR83 and its natural antisense transcript DHPS in gastric cancer. Cell Res 22: 1374**
Pubmed: [Author and Title](#)
Google Scholar: [Author Only](#) [Title Only](#) [Author and Title](#)
- Suenaga Y, Islam SR, Alagu J, Kaneko Y, Kato M, Tanaka Y, Kawana H, Hossain S, Matsumoto D, Yamamoto M, et al (2014) NCYM, a cis-**

antisense gene of MYCN, encodes a de novo evolved protein that inhibits GSK3 β resulting in the stabilization of MYCN in human neuroblastomas. *PLoS Genet* 10: e1003996

Pubmed: [Author and Title](#)

Google Scholar: [Author Only](#) [Title Only](#) [Author and Title](#)

Swiezewski S, Liu F, Magusin A, Dean C (2009) Cold-induced silencing by long antisense transcripts of an Arabidopsis polycomb target. *Nature* 462: 799-802

Pubmed: [Author and Title](#)

Google Scholar: [Author Only](#) [Title Only](#) [Author and Title](#)

Tilgner H, Raha D, Habegger L, Mohiuddin M, Gerstein M, Snyder M (2013) Accurate identification and analysis of human mRNA isoforms using deep long read sequencing. *G3: Genes Genom Genet* 3: 387-397

Pubmed: [Author and Title](#)

Google Scholar: [Author Only](#) [Title Only](#) [Author and Title](#)

Tress ML, Abascal F, Valencia A (2016) Alternative splicing may not be the key to proteome complexity. *Trends Biochem Sci* 42: 98-110

Pubmed: [Author and Title](#)

Google Scholar: [Author Only](#) [Title Only](#) [Author and Title](#)

Volkening JD, Bailey DJ, Rose CM, Grimsrud PA, Howespodoll M, Venkateshwaran M, Westphall MS, Ané JM, Coon JJ, Sussman MR (2012) A proteogenomic survey of the Medicago truncatula genome. *Mol Cell Proteomics* 11: 933-944

Pubmed: [Author and Title](#)

Google Scholar: [Author Only](#) [Title Only](#) [Author and Title](#)

Wade JT, Grainger DC (2014) Pervasive transcription: illuminating the dark matter of bacterial transcriptomes. *Nat Rev Microbiol* 12: 647-653

Pubmed: [Author and Title](#)

Google Scholar: [Author Only](#) [Title Only](#) [Author and Title](#)

Wang B, Tseng E, Regulski M, Clark TA, Hon T, Jiao Y, Lu Z, Olson A, Stein JC, Ware D (2016) Unveiling the complexity of the maize transcriptome by single-molecule long-read sequencing. *Nat Commun* 7: 11708

Pubmed: [Author and Title](#)

Google Scholar: [Author Only](#) [Title Only](#) [Author and Title](#)

Wang H, Chung PJ, Liu J, Jang IC, Kean MJ, Xu J, Chua NH (2014) Genome-wide identification of long noncoding natural antisense transcripts and their responses to light in Arabidopsis. *Genome Res* 24: 444-453

Pubmed: [Author and Title](#)

Google Scholar: [Author Only](#) [Title Only](#) [Author and Title](#)

Wang M, Wang P, Liang F, Ye Z, Li J, Shen C, Pei L, Wang F, Hu J, Tu L, et al (2018) A global survey of alternative splicing in allopolyploid cotton: landscape, complexity and regulation. *New Phytol* 217: 163-178

Pubmed: [Author and Title](#)

Google Scholar: [Author Only](#) [Title Only](#) [Author and Title](#)

Wang W, Mauleon R, Hu Z, Chebotarov D, Tai S, Wu Z, Li M, Zheng T, Fuentes RR, Zhang F, et al (2018) Genomic variation in 3,010 diverse accessions of Asian cultivated rice. *Nature* 557: 43-49

Pubmed: [Author and Title](#)

Google Scholar: [Author Only](#) [Title Only](#) [Author and Title](#)

Wang Z, Ji H, Yuan B, Wang S, Su C, Yao B, Zhao H, Li X (2015) ABA signalling is fine-tuned by antagonistic HAB1 variants. *Nat commun* 6: 8138

Pubmed: [Author and Title](#)

Google Scholar: [Author Only](#) [Title Only](#) [Author and Title](#)

Weirather JL, Afshar PT, Clark TA, Tseng E, Powers LS, Underwood JG, Zabner J, Korlach J, Wong WH, Au KF (2015) Characterization of fusion genes and the significantly expressed fusion isoforms in breast cancer by hybrid sequencing. *Nucleic Acids Res* 43: e116

Pubmed: [Author and Title](#)

Google Scholar: [Author Only](#) [Title Only](#) [Author and Title](#)

Wek RC, Hatfield GW (1986) Nucleotide sequence and in vivo expression of the ilvY and ilvC genes in Escherichia coli K12. Transcription from divergent overlapping promoters. *J Biol Chem* 261: 2441-2450

Pubmed: [Author and Title](#)

Google Scholar: [Author Only](#) [Title Only](#) [Author and Title](#)

Werner A (2005) Natural antisense transcripts. *RNA Biol* 2: 53-62

Pubmed: [Author and Title](#)

Google Scholar: [Author Only](#) [Title Only](#) [Author and Title](#)

Will CL, Luhrmann R (2011) Spliceosome structure and function. *Cold Spring Harb Perspect Biol* 3: a003707

Pubmed: [Author and Title](#)

Google Scholar: [Author Only](#) [Title Only](#) [Author and Title](#)

Wong F, Yuh ZT, Schaefer EL, Roop BC, Ally AH (1987) Overlapping transcription units in the transient receptor potential locus of Drosophila melanogaster. *Somat Cell Mol Genet* 13: 661-669

Pubmed: [Author and Title](#)

Downloaded from on February 28, 2020 - Published by www.plantphysiol.org
Copyright © 2019 American Society of Plant Biologists. All rights reserved.

Google Scholar: [Author Only](#) [Title Only](#) [Author and Title](#)

Wu DD, Irwin DM, Zhang YP (2011) De novo origin of human protein-coding genes. PLoS Genet 7: e1002379

Pubmed: [Author and Title](#)

Google Scholar: [Author Only](#) [Title Only](#) [Author and Title](#)

Xu J, Wang Q, Freeling M, Zhang X, Xu Y, Mao Y, Tang X, Wu F, Lan H, Cao M, et al (2017) Natural antisense transcripts are significantly involved in regulation of drought stress in maize. Nucleic Acids Res 45: 5126-5141

Pubmed: [Author and Title](#)

Google Scholar: [Author Only](#) [Title Only](#) [Author and Title](#)

Yuan C, Wang J, Harrison AP, Meng X, Chen D, Chen M (2015) Genome-wide view of natural antisense transcripts in Arabidopsis thaliana. DNA Res 22: 233-243

Pubmed: [Author and Title](#)

Google Scholar: [Author Only](#) [Title Only](#) [Author and Title](#)

Zdraviko J L, Reinhard L, Christina F, Andrea B (2005) Evolutionary conservation of minor U12-type spliceosome between plants and humans. RNA 11: 1095-1107

Pubmed: [Author and Title](#)

Google Scholar: [Author Only](#) [Title Only](#) [Author and Title](#)

Zhang B, Wang J, Wang X, Zhu J, Liu Q, Shi Z, Chambers MC, Zimmerman LJ, Shaddox KF, Kim S, et al (2014) Proteogenomic characterization of human colon and rectal cancer. Nature 513: 382-387

Pubmed: [Author and Title](#)

Google Scholar: [Author Only](#) [Title Only](#) [Author and Title](#)

Zhang G, Sun M, Wang J, Lei M, Li C, Zhao D, Huang J, Li W, Li S, Li J, et al (2019) PacBio full-length cDNA sequencing integrated with RNA-seq reads drastically improves the discovery of splicing transcripts in rice. Plant J 97: 296-305

Pubmed: [Author and Title](#)

Google Scholar: [Author Only](#) [Title Only](#) [Author and Title](#)

Zhang H, Liu T, Zhang Z, Payne SH, Zhang B, McDermott JE, Zhou JY, Petyuk VA, Chen L, Ray D, et al (2016) Integrated proteogenomic characterization of human high-grade serous ovarian cancer. Cell 166: 755-765

Pubmed: [Author and Title](#)

Google Scholar: [Author Only](#) [Title Only](#) [Author and Title](#)

Zhang X, Lii Y, Wu Z, Polishko A, Zhang H, Chinnusamy V, Lonardi S, Zhu JK, Liu R, Jin H (2013) Mechanisms of small RNA generation from cis-NATs in response to environmental and developmental cues. Mol Plant 6: 704-715

Pubmed: [Author and Title](#)

Google Scholar: [Author Only](#) [Title Only](#) [Author and Title](#)

Zhu FY, Chen MX, Ye NH, Shi L, Ma KL, Yang JF, Cao YY, Zhang YJ, Yoshida T, Fernie AR, et al (2017) Proteogenomic analysis reveals alternative splicing and translation as part of the abscisic acid response in Arabidopsis seedlings. Plant J 91: 518-533

Pubmed: [Author and Title](#)

Google Scholar: [Author Only](#) [Title Only](#) [Author and Title](#)

Zhu F, Chen MX, Chan W, Yang F, Tian Y, Song T, Xie LJ, Zhou Y, Xiao S, Zhang J (2018) SWATH-MS quantitative proteomic investigation of nitrogen starvation in Arabidopsis reveals new aspects of plant nitrogen stress responses. Journal of Proteomics 187: 161-170

Pubmed: [Author and Title](#)

Google Scholar: [Author Only](#) [Title Only](#) [Author and Title](#)